Next-to-leading-order corrections to inclusive hadron photoproduction

L. E. Gordon
Institut für Physik, Universität Dortmund, D-44221 Dortmund, Germany
(Received 22 February 1994; revised manuscript received 22 July 1994)

We present a complete calculation of next-to-leading-order corrections to inclusive hadron photoproduction. We take into account all contributions from resolved and unresolved photons and apply the results to π^0 production at CERN LEP 2 as well as at the DESY ep collider HERA where we study in detail the scale dependence of the cross section. In addition compact analytical expressions for the matrix elements for all the direct contributions to both cross sections are presented. We also make a comparison with existing single tag data on inclusive charged hadron production.

PACS number(s): 12.38.Bx, 13.60.Le, 13.60.Rj, 13.65.+i

I. INTRODUCTION

Recently, new experimental data on the photoproduction of hadrons have started to appear from both the KEK e^+e^- collider at TRISTAN [1] and the DESY ep collider HERA [2]. The current data exist at relatively low p_T only, but it is still both necessary and desirable that they be confronted with next-to-leading-order (NLO) calculations whenever possible in order to provide quantitative tests of perturbative QCD. It is also anticipated that the range and quality of the data will soon be extended and improved at both HERA and the CERN e^+e^- collider LEP 2. Furthermore, it is hoped that the photoproduction of prompt photons will be studied at HERA very soon [3–5] and π^0 photoproduction will be an important background to these processes. Inclusive hadron production is also in itself interesting since it can and has been used to tie down important QCD parameters such as structure functions and the much neglected fragmentation functions. With this in mind we have calculated all the higher-order [$O(\alpha_s)$] corrections to the photoproduction of inclusive hadrons relevant for both e^+e^- and ep machines. The inclusive hadron photoproduction cross section in e^+e^- collisions has been previously measured [6–8], but at rather low center-of-mass (c.m.) energies. Comparisons between theoretical predictions and some of these data have shown discrepancies which have been attributed to various causes. We shall discuss this point more extensively later.

It is customary when considering photoproduction processes to separate those contributions to the cross section where the photon interacts via its pointlike electromagnetic coupling from those where it does so via its partonic constituents. This defines the so-called direct and resolved processes [9]. When considering γp interactions, for example, the labels direct and resolved are sufficient to define the classes of processes, but in the case of $\gamma\gamma$ collisions there is the additional case where both photons interact via pointlike couplings. In this paper we will adopt the convention whereby, when discussing $\gamma\gamma$ collisions, we identify the three following classes of contributions to the inclusive hadron cross section: the direct contributions where the photons couple directly to the quarks produced in the hard scattering process [Fig. 1(a)], the once-resolved contributions where one photon is resolved into its partonic constituents before interacting with the other [Fig. 1(b)], and the twice-resolved contributions where both photons interact via their partonic constituents [Fig. 1(c)]. In the first case there are no hadronic fragments or spectator jets from either photon, whereas in the latter two cases such fragments are produced in each event, in one or both beam directions, for once- and twice-resolved processes, respectively. When we discuss γp processes, we will use the usual labels of direct and resolved contributions as defined in Fig. 2. As much as possible, we will keep the discussions of the two reactions separate.

It may be possible for the photon fragments produced in the reactions to be tagged, thereby providing a means of separating the three classes of processes, but as has been discussed elsewhere [10–13], this simple separation is no longer so clear from a theoretical point of view

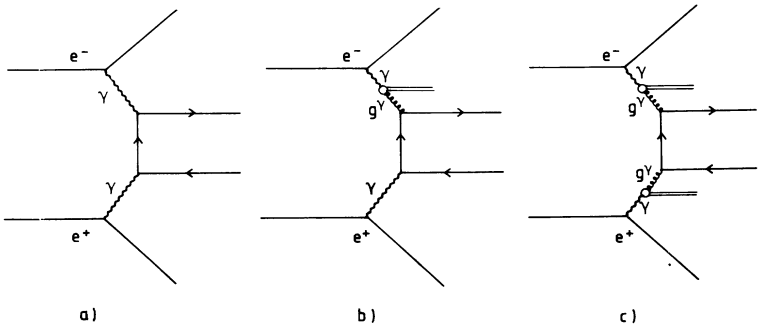

FIG. 1. Examples of (a) direct, (b) once-resolved, and (c) twice-resolved processes in quasireal $\gamma\gamma$ scattering at e^+e^- machines.

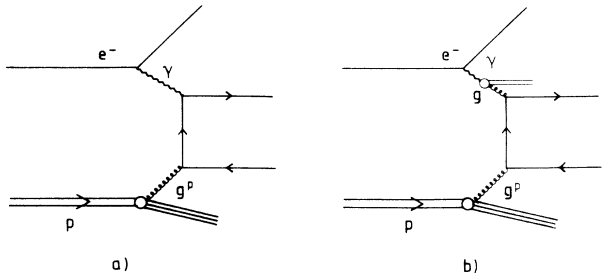

FIG. 2. Examples of (a) direct and (b) resolved processes in quasireal γp scattering at HERA.

when higher-order (HO) corrections are taken into account, since a residual scale dependence is introduced into each class of process which is only canceled by a similar dependence in one of the other classes. Nevertheless, the artificial separation can still be made as long as care is taken that the scales are not mismatched when the sum is taken for the full inclusive cross section. We will discuss this point in more detail in Sec. II.

The relevant matrix elements to perform a complete calculation, although all obtained before [14,16], to our knowledge, are not all freely available. This applies specifically to the case of one pointlike photon. We have thus calculated all the matrix elements involving the direct processes, i.e., one or two pointlike couplings of the photon in the initial state, again and present the results in a compact form in Appendixes A and B for the convenience of future users. We discuss the details of our calculation in Sec. II. We will use the integrated matrix elements of Ref. [16], which are available in a FORTRAN code, for the twice-resolved or resolved processes.

In the case of photoproduction of π^0 at HERA, a calculation has been published recently [17] where the matrix elements of Ref. [16] were also used to obtain the resolved contributions, but the direct contributions were estimated in leading order (LO) only, and fragmentation functions evolved in LO only were used. Recently, charged hadron production at HERA has been studied by the same authors where the direct contributions are also included using the matrix elements of Ref. [14], obtained via a private communication [18]. In the case of π^0 production at LEP 2, to our knowledge no calculation has yet been performed, and the results presented here should in any case be the first full NLO calculation.

At this stage a complete and consistent NLO calculation can be performed since recently parametrizations of the fragmentation functions for partons into a π^0 have, for the first time, become available in NLO [19]. In this calculation we make use of the proton distribution functions of Ref. [20] and use parton distributions for the photon from Refs. [21,22], which are available in both LO and NLO.

The outline of this paper is as follows. In Sec. II we develop the theoretical background to the calculation. In Sec. III we discuss the details of our calculation of the matrix elements. In Sec. IV we present our numerical results and make a comparison with the Mark II single tagged data, and finally in Appendixes A and B we list the matrix elements.

II. THEORETICAL BACKGROUND

A. Inclusive π^0 cross section at LEP 2 and HERA

We wish to study the reactions $e^-(P_1)+e^+(P_2)\to\pi^0(P_h)+X$ and $e^-(P_1)+p(P_2)\to\pi^0(P_h)+X$ at LEP 2 and HERA, respectively, where X includes all unobserved reaction products including the scattered leptons. At LEP 2 we can write the cross section as

$$E\frac{d\sigma}{d^3p}=\frac{1}{\pi S}\sum_{i,j,l}\int_{1-V+VW}^{1}\frac{dz}{z^2}\int_{VW/z}^{1-(1-V)/z}\frac{dv}{1-v}\int_{VW/vz}^{1}\frac{dw}{w}f_-(x_1,M^2)f_+(x_2,M^2)$$
$$\times D_l^{\pi^0}(z,M_F^2)\left[\frac{1}{v}\frac{d\hat{\sigma}_{ij\to l}}{dv}\delta(1-w)+\frac{\alpha_s(\mu^2)}{2\pi}K_{ij\to l}(\hat{s},v,w,\mu^2,M^2,M_F^2)\right], \quad (1)$$

where $S=(P_1+P_2)^2$, $T=(P_1-P_h)^2$, $U=(P_2-P_h)^2$, $x_1=VW/vwz$, $x_2=(1-V)/z(1-v)$, and $s=x_1x_2S$. The Mandelstam variables are defined as usual with uppercase letters defined for the electron-positron system and lowercase letters for the parton-parton system. $f_-(x_1,M^2)$ and $f_+(x_2,M^2)$ represent the probability of finding a parton, including a photon, in the electron and positron with momentum fractions x_1 and x_2, respectively, at scale M^2, i.e., the "electron structure functions," while $D_l^{\pi^0}(z,M_F^2)$ is the usual fragmentation function for parton l into a π^0. The variables V, W, v, and w are defined in terms of the Mandelstam variables by $V=1+T/S$, $W=-U/(S+T)$, $v=1+t/s$, and $w=-u/(s+t)$. The first term in the square brackets is the LO contribution to the hard subprocess scattering cross section, while the second term in the NLO contribution.

We make use of the Weizsäcker-Williams approximation [23] to estimate the flux of quasireal photons from the electron and positron beams. In order to ensure that the photons participating in the reaction are almost real, thereby justifying the use of the real photon structure functions, we restricted the angle for the scattered electrons and positrons to be less than $\theta=5^\circ$ in the formula

$$f_{\gamma/e}(y)=\frac{\alpha_{\rm em}}{2\pi}\left[\frac{1+(1-y)^2}{y}\right]2\ln\frac{E_e\theta}{m_e}. \quad (2)$$

Here E_e is the electron and/or positron beam energies, m_e their masses, and $\alpha_{\rm em}$ the electromagnetic coupling constant. We present results for a fixed beam energy $E_e=100$ GeV, relevant for LEP 2. According to the results of Ref. [24], the error introduced by using this approximation at these small angles should not be greater than a few percent.

The structure functions for finding a particular parton in the electron or positron, $f_{-/+}(x_i, Q^2)$, with momentum fraction x_i is given in the Weizsäcker-Williams approximation by a convolution with the function $f_{\gamma/e}(y)$ given in Eq. (2):

$$f_i(x_i, Q^2) = \int_{x_i}^1 \frac{dy}{y} f_{\gamma/e}(y) f^\gamma\left(\frac{x_i}{y}, Q^2\right) , \tag{3}$$

where f^γ is the photon structure function. Thus the photon structure functions are evaluated at $x_i^\gamma = x_i/y_i$, and in the parton-parton c.m. system the Mandelstam variable $\hat{s}$ is given by

$$\hat{s} = x_1^\gamma x_2^\gamma y_1 y_2 S . \tag{4}$$

When one or both photons participate directly in the hard scattering, then the appropriate structure function(s) must be modified. This is achieved by replacing the photon structure function(s) by a delta function $\delta(1 - x_i/y)$ in Eq. (3). This replaces Eq. (3) by $f_i(x_i, Q^2) = f_{\gamma/e}(x_i)$.

The reaction we will study at HERA can be written in a similar form to Eq. (1), but now we must replace the "positron structure function" by the proton distribution function $f^p(x, M^2)$. The equation becomes

$$E\frac{d\sigma}{d^3p} = \frac{1}{\pi S}\sum_{i,j,l}\int_{1-V+VW}^1 \frac{dz}{z^2}\int_{VW/z}^{1-(1-V)/z}\frac{dv}{1-v}\int_{VW/vz}^1 \frac{dw}{w} f_-(x_1, M^2) f^p(x_p, M^2)$$
$$\times D_l^{\pi^0}(z, M_F^2)\left[\frac{1}{v}\frac{d\hat{\sigma}_{ij\to l}}{dv}\delta(1-w) + \frac{\alpha_s(\mu^2)}{2\pi}K_{ij\to l}(\hat{s}, v, w, \mu^2, M^2, M_F^2)\right] , \tag{5}$$

and x_2^γ is set to x_p while y_2 is set to 1 in Eq. (4).

B. Real photon in hard scattering processes

In this section we give an outline of the unique behavior of the photon in hard scattering reactions. In particular, we explain why the separation of the cross section into resolved and direct contributions is no longer well defined when NLO corrections are taken into consideration. We present the discussion for $\gamma\gamma$ scattering, but note that the argument is equally valid for γ-hadron scattering, although then the starting point is, conceptually at least, equivalent to the once-resolved case.

The QCD factorization theorem [25] provides us with a prescription for calculating the cross section for the production of a hadron H from the high-energy collision of two incoming hadrons A and B starting with the schematic parton model formula

$$d\sigma^{AB\to HX} = \sum_{a,b,c}\int dx_1 \int dx_2 \int dz\, f^A(x_1) f^B(x_2)$$
$$\times d\hat{\sigma}^{ab\to cX} D_{H/c}(z) . \tag{6}$$

The cross section is thus factorized into a short-distance "hard" scattering cross section $d\hat{\sigma}$ which is calculable in perturbative QCD and the long-distance structure and fragmentation functions $f^A(x_1)$, $f^B(x_2)$, and $D_{H/c}(z)$, respectively, which are not calculable in perturbative QCD. The summation in Eq. (6) is to be taken over all possible parton types, including in our case photons, which may participate in the hard scattering reaction.

When radiative corrections are taken into account, the structure and fragmentation functions acquire a scale dependence, which is typically taken as approximately the order of magnitude of the transverse momentum squared (p_T^2) of the produced hadron, but is not uniquely defined in the theory. Given measured values for these functions at some arbitrary scale Q_0^2, perturbative QCD can be used, via the Altarelli-Parisi evolution equations [26], to predict their values at any higher scale Q^2. We thus have a clear recipe for calculating the cross section which consists of combining hard scattering cross sections with evolved structure and fragmentation functions according to Eq. (6).

In LO in QCD the structure and fragmentation functions are evolved from Q_0^2 using the LO Altarelli-Parisi evolution equations and the hard scattering cross section is calculated in the Born approximation; i.e., only $2 \to 2$ scattering is explicitly considered. The contributions from gluon radiation off quarks and gluon (or photon) splitting into quark-antiquark pairs are implicitly taken into account in the collinear limit only. This procedure represents an all-orders calculation, but one where only leading logarithms in the perturbation series are retained and summed [27]. A consequence of this treatment is that there is no factorization scheme dependence in the cross section because no explicit factorization procedure is carried out. Applied to the case of $\gamma\gamma$ scattering, the schematic formula [Eq. (6)] becomes

$$d\hat{\sigma}^{\gamma\gamma\to HX} = \int dz \left[\sum_c d\hat{\sigma}^{\gamma\gamma\to cX} + \sum_{a,c}\int dx_1 f_a^\gamma(x_1, M^2) d\hat{\sigma}^{a\gamma\to cX} + \sum_{b,c}\int dx_2 f_b^\gamma(x_2, M^2) d\hat{\sigma}^{\gamma b\to cX}\right.$$
$$\left. + \sum_{a,b,c}\int dx_1 f_a^\gamma(x_1, M^2)\int dx_2 f_b^\gamma(x_2, M^2) d\hat{\sigma}^{ab\to cX}\right] D_{H/c}(z, M_F^2) . \tag{7}$$

The first term is the direct contribution, while the second and third terms are the once- and twice-resolved contributions, respectively. It should be stressed that, in leading order, Eq. (7) represents a calculation where all the three contributions are $O(\alpha_{\rm em}^2)$. This is despite the fact that the hard scattering cross sections for the three classes of processes are $O(\alpha_{\rm em}^2)$, $O(\alpha_{\rm em}\alpha_s)$, and $O(\alpha_s^2)$ for the direct and once- and twice-resolved processes, respectively (see Appendixes A and B). The reason for this is the unique dependence of the photon structure function on the coupling constants [28]. It is proportional to $\alpha_{\rm em}/\alpha_s$ and can cancel one (two) powers of α_s in the once- (twice-) resolved processes. Note also that the direct process is a pure QED process involving only electromagnetic couplings in LO. The presence of the QCD processes in Eq. (7) is a direct consequence of the coupling of the photon to a $q\bar{q}$ pair *before* interaction with the other photon.

One very important feature of the LO calculation as outlined above is that the hard subprocess cross sections, except for the direct case, are only scale dependent via the renormalization scale μ^2, through the LO QCD coupling constant

$$\alpha_s(\mu^2) = \frac{4\pi}{\beta_0 \ln \frac{\mu^2}{\Lambda^2}} , \tag{8}$$

where $\beta_0 = 11 - \frac{2}{3}N_f$, Λ is the QCD mass scale, and N_f is the number of active quark flavors. The full cross section is of course dependent on the choice of the scales M^2 and M_F^2, where the collinear singularities, implicit in the LO treatment, are absorbed into the structure and fragmentation functions, respectively. This treatment, in which only leading logarithmic terms are retained in each part of the factorized cross section, leads to a strong dependence of the cross section on the choice of these arbitrary scales. This is one of the main drawbacks of the LO calculation. As we shall show below, performing the calculation in NLO usually leads to a significant reduction in this scale dependence as a result of a scale dependence cancellation mechanism which works as follows. As in Eq. (1), the hard scattering cross section in NLO is written as

$$d\hat{\sigma}(\mathrm{LO}) + \alpha_s K(\hat{s}, v, w, \mu^2, M^2, M_F^2) , \tag{9}$$

where the explicit dependence on M^2 in the second term cancels to some extent the M^2 dependence of the LO cross section [Eq. (7)] as a result of the structure function dependences on M^2 via the Altarelli-Parisi evolution equations. A scale cancellation mechanism also exists for the other scales, but since these are the same as for hadron-hadron processes and we are mainly concerned with the unique behavior of the photon, we do not discuss them here. As we shall see in the case of photoproduction processes, the simple separation into direct and resolved photon contributions, which was well defined in LO, is no longer so well defined.

Consider what happens when $O(\alpha_s)$ radiative gluon corrections are calculated for the direct contribution in Eq. (7), where c is a quark. First of all, we have the interference between the virtual diagrams in Fig. 3(b) and the lowest-order Born diagrams in Fig. 3(a). The calculation is performed in $4-2\epsilon$ dimensions [29], where all ultraviolet, collinear, and infrared (soft) singularities encountered show up as poles in ϵ. Singularities from simultaneously soft and collinear regions of phase space are represented as double $(1/\epsilon^2)$ poles. First, the ultraviolet poles are subtracted off by choosing an appropriate renormalization scheme. In our calculation we use the modified minimal subtraction $\overline{\rm MS}$ renormalization scheme, where the poles are subtracted along with attendant Euler constant γ_E and $\ln 4\pi$ [30].

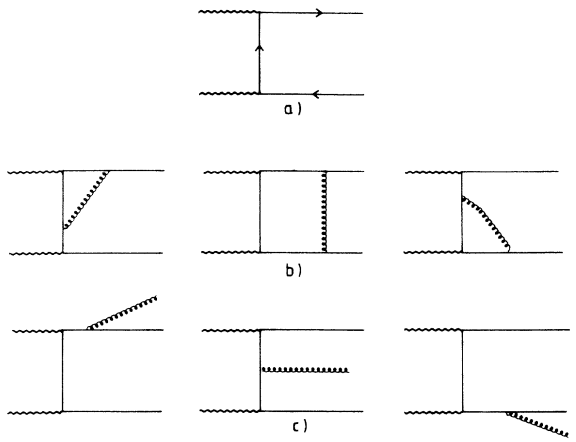

FIG. 3. (a) Lowest-order (Born) diagram contributing to $\gamma\gamma$ scattering. Examples of (b) virtual and (c) real emission diagrams contributing to the $\gamma\gamma$ scattering process at $O(\alpha_s)$.

The next step is to calculate the real gluon emission processes in Fig. 3(c). The method for performing this will be outlined in the next section. Here we only consider the structure of the results. Performing the calculation in $4-2\epsilon$ dimensions, all soft and collinear singularities are exposed as poles in ϵ. Adding the result to the virtual corrections leads to a cancellation of all soft and double poles. The remaining collinear poles must now be factored into the structure and fragmentation functions at scales M^2 and M_F^2 (in the $\overline{\rm MS}$ scheme in our case). This procedure creates a dependence of the hard cross section on the scales M^2 and M_F^2, which are shown in Eq. (9) in the second term.

One must recall that the process we are considering here is the direct scattering of two photons and that the scale M^2 corresponds to the scale at which the photon distribution function is tested. This clearly means that in NLO the direct processes are no longer independent of the once-resolved processes. A similar argument would show that the same situation is encountered between the once- and twice-resolved processes.

To be more specific, we consider now in detail the cancellation mechanism for the scale dependence and show explicitly the interdependences of the various contributing processes. In NLO we can rewrite the schematic process in Eq. (7) in the form

$$d\hat{\sigma}^{\gamma\gamma\to HX} = \int dz \left[\sum_c \left\{ d\hat{\sigma}^{\gamma\gamma\to cX} + \frac{\alpha_s(\mu^2)}{2\pi} K^{\gamma\gamma\to cX}(\hat{s},v,w,M^2,M_F^2) \right\} + \sum_{a,c} \int dx_1 f_a^\gamma(x_1,M^2) \left\{ d\hat{\sigma}^{a\gamma\to cX} + \frac{\alpha_s(\mu^2)}{2\pi} K^{a\gamma\to cX}(\hat{s},v,w,\mu^2,M^2,M_F^2) \right\} + \sum_{b,c} \int dx_2 f_b^\gamma(x_2,M^2) \left\{ d\hat{\sigma}^{\gamma b\to cX} + \frac{\alpha_s(\mu^2)}{2\pi} K^{\gamma b\to cX}(\hat{s},v,w,\mu^2,M^2,M_F^2) \right\} + \sum_{a,b,c} \int dx_1 f_a^\gamma(x_1,M^2) \int dx_2 f_b^\gamma(x_2,M^2) \left\{ d\hat{\sigma}^{ab\to cX} + \frac{\alpha_s(\mu^2)}{2\pi} K^{ab\to cX}(\hat{s},v,w,\mu^2,M^2,M_F^2) \right\} \right] \times D_{H/c}(z,M_F^2) , \tag{10}$$

using the same notation as before. Note that, for brevity, we have not explicitly written out the dependences of the hard subprocess cross sections on the couplings $\alpha_{\rm em}$ and α_s, but only the relative $O(\alpha_s)$ dependences of the HO processes with respect to their LO counterparts. As stated above, we consider dependence on the initial state factorization scale M^2 only since the dependence on μ^2 and M_F^2 is similar to the case for purely hadronic processes.

Neglecting the M^2-independent LO contribution to the direct process, as a result of factorization process, we can rewrite the three contributions to the hard subprocess cross sections in the forms

$$d\hat{\sigma}^{\gamma\gamma} = \frac{\alpha_{\rm em}}{2\pi} \{ P_{i\gamma} * d\hat{\sigma}^{i\gamma} + P_{j\gamma} * d\hat{\sigma}^{\gamma j} \} \ln \frac{\hat{s}}{M^2} + k^{\gamma\gamma}(\hat{s},v,w,M_F^2) , \tag{11}$$

$$d\hat{\sigma}^{i\gamma} = f_i^\gamma * \left[d\hat{\sigma}^{i\gamma} + \left\{ \frac{\alpha_{\rm em}}{2\pi} P_{j\gamma} * d\hat{\sigma}^{ij} + \frac{\alpha_s}{2\pi} P_{ij} * d\hat{\sigma}^{j\gamma\to cX} \right\} \ln \frac{\hat{s}}{M^2} + k^{i\gamma}(\hat{s},v,w,\mu^2,M_F^2) \right] , \tag{12}$$

and a similar form for $d\hat{\sigma}^{\gamma j}$, plus

$$d\hat{\sigma}^{ij} = f_i^\gamma f_j^\gamma ** \left[d\hat{\sigma}^{ij} + \left\{ \frac{\alpha_{\rm em}}{2\pi} P_{ik} * d\hat{\sigma}^{kj} + \frac{\alpha_s}{2\pi} P_{jl} * d\hat{\sigma}^{il} \right\} \ln \frac{\hat{s}}{M^2} + k^{ij}(\hat{s},v,w,\mu^2,M_F^2) \right] , \tag{13}$$

where the general convolution is represented by $*$, the terms k represent the HO contributions independent of M^2, and summation over repeated indices is implied. We have written explicitly only the coupling constants connected with the splitting functions and absorbed the others into the structure functions and hard subprocess cross sections.

To see the variation with M^2, as an example, we differentiate Eqs. (11) and (12) with respect to $\ln M^2$ and obtain

$$\frac{\partial(d\hat{\sigma}^{\gamma\gamma})}{\partial \ln M^2} = -\frac{\alpha_{\rm em}}{2\pi} \{ P_{i\gamma} * d\sigma^{i\gamma} + P_{j\gamma} * d\hat{\sigma}^{\gamma j} \} \tag{14}$$

and

$$\frac{\partial(d\hat{\sigma}^{i\gamma})}{\partial \ln M^2} = \left\{ \frac{\alpha_{\rm em}}{2\pi} P_{i\gamma} + \frac{\alpha_s}{2\pi} P_{ij} * f_j^\gamma \right\} * \{ d\hat{\sigma}^{i\gamma} + K^{i\gamma} \} + f_i^\gamma * \frac{\partial K^{i\gamma}}{\partial \ln M^2} , \tag{15}$$

where Eq. (15) follows from the inhomogeneous evolution equation for the photon structure function

$$\frac{\partial f_i^\gamma}{\partial \ln M^2} = \frac{\alpha_{\rm em}}{2\pi} P_{i\gamma} + \frac{\alpha_s}{2\pi} P_{ij} * f_j^\gamma . \tag{16}$$

Thus we see that the scale dependence of the direct contribution is canceled by a corresponding dependence in the once-resolved process, controlled by the inhomogeneous term in the evolution equation for the photon structure function [first term in Eq. (16)]. We have not explicitly shown the corresponding cancellation between the once- and twice-resolved processes which are controlled by the homogeneous term in Eq. (16), but an examination of Eqs. (12) and (13) will show that this cancellation does indeed occur.

The scale dependence cancellation mechanism between the once- and twice-resolved processes is of similar form to that between the direct and resolved contributions in γ-hadron interactions and were considered in Refs. [11] and [13]. In the former reference it was shown explicitly how the scale dependence of the NLO direct component is canceled by a similar dependence in the resolved contribution to $O(\alpha_{\rm em}\alpha_s^2)$.

This concludes our discussion of the separation of direct and resolved contributions to photoproduction where

we have demonstrated the difficulties involved in this naive separation beyond the leading order. We now give a brief discussion of the standard methods for integrating the matrix elements.

III. INTEGRATION OF MATRIX ELEMENTS

We consider first the direct contributions to $\gamma\gamma$ scattering. The virtual corrections can be obtained from many sources [11,31–33] or even, in principle, from virtual corrections to processes such as $q\bar{q} \to \gamma g$ which can be found in the literature, but they are also quite simple to calculate. We checked our results against those of Ref. [33] after removing non-Abelian couplings and adjusting color factors and found complete agreement. We do not give the results here since they were already presented in Ref. [15]. All the relevant integrals needed to perform this calculation can be found in Ref. [34].

The $2 \to 3$ process we need to consider is

$$\gamma\gamma \to q\bar{q}g \ . \tag{17}$$

The matrix element was obtained from Ref. [35], where it was calculated for the process $gg \to q\bar{q}\gamma$ by first crossing and then removing the non-Abelian couplings by setting N_C to zero and finally adjusting color factors. The next step is to integrate over the phase space of the unobserved final state partons. Thus we wish to calculate the cross sections for the processes

$$\begin{aligned} &\gamma\gamma \to q + X \ , \\ &\gamma\gamma \to \bar{q} + X \ , \\ &\gamma\gamma \to g + X \ . \end{aligned} \tag{18}$$

Clearly, the first two processes will give identical results. The method for performing the phase space integrals for the matrix elements has been extensively discussed elsewhere and can be found, for example, in [36].

The phase space integrals for $\gamma\gamma \to q(\bar{q}) + X$ yield results containing $1/\epsilon^2$ as well as $1/\epsilon$ poles, while for $\gamma\gamma \to g + X$ only the latter are produced. The latter process has no virtual contributions at $O(\alpha_s)$, and thus integration of the $2 \to 3$ matrix elements and factorization of the collinear singularities completes the calculation. For the inclusive (anti)quark production processes, the virtual corrections are added to the $2 \to 3$ contributions, in which case all $1/\epsilon^2$ poles immediately cancel out. The remaining collinear poles must now be factorized as discussed in the previous section. As previously stated, we perform all factorizations in the $\overline{\text{MS}}$ scheme.

We take this opportunity to note that for a consistent implementation of the $\overline{\text{MS}}$ scheme the spin averaging for the incoming photons and gluons should be taken as $1/[2(1-\epsilon)]$ and not $\frac{1}{2}$ as was done in Ref. [14]. Throughout our calculation we use the former choice and indicate the difference between the two by the parameter λ (Appendixes A and B). The choice $\lambda = 1$ corresponds to the $\overline{\text{MS}}$ scheme.

The remaining $2 \to 3$ processes calculated in this paper all contribute to the once-resolved processes. They are

$$\begin{aligned} &\gamma q \to g + g + q \ , \\ &\gamma q \to q + q + \bar{q} \ , \\ &\gamma q \to q + q' + \bar{q}' \ , \\ &\gamma g \to g + q + \bar{q} \ , \end{aligned} \tag{19}$$

which are integrated to give the inclusive processes

$$\begin{aligned} &\gamma q \to q + X \ , \\ &\gamma q \to g + X \ , \\ &\gamma g \to q + X \ , \\ &\gamma g \to g + X \ , \\ &\gamma q \to \bar{q} + X \ , \\ &\gamma q \to q' + X \ , \end{aligned} \tag{20}$$

where antiquarks are also implied. The first three processes all have contributions from virtual diagrams. The virtual corrections to the processes

$$\gamma q \to qg, \quad \gamma g \to q\bar{q}$$

where calculated in Refs. [14] and [33], respectively. We use these results in our calculation after checking that crossing the results of the latter yields exactly the results given in the former reference. The unintegrated $2 \to 3$ matrix elements calculated in Ref. [35] were again crossed to obtain those for the processes in Eq. (19).

The procedure for integration of the matrix elements and factorizing the collinear singularities is again the same as outlined above, and our final results are presented in Appendixes A and B, where they are given in the form

$$\begin{aligned} \hat{s}\frac{d\hat{\sigma}}{dv\,dw} &= \frac{\hat{s}v}{2\pi\alpha_s\alpha_{\rm em}} K(\hat{s}, v, w, \mu^2, M^2, M_F^2) \\ &= \left[c_1 + \tilde{c}_1 \ln\left(\frac{M^2}{\hat{s}}\right) + \tilde{\tilde{c}}_1 \ln\left(\frac{M_F^2}{\hat{s}}\right) + \hat{c}_1 \ln\left(\frac{\mu^2}{\hat{s}}\right)\right]\delta(1-w) \\ &\quad + \left[c_2 + \tilde{c}_2 \ln\left(\frac{M^2}{\hat{s}}\right) + \tilde{\tilde{c}}_2 \ln\left(\frac{M_F^2}{\hat{s}}\right)\right]\frac{1}{(1-w)_+} + c_3\left[\frac{\ln(1-w)}{1-w}\right]_+ \\ &\quad + c_5 \ln v + c_6 \ln(1-vw) + c_7 \ln(1-v+vw) + c_8 \ln(1-v) + c_9 \ln w \\ &\quad + c_{10} \ln(1-w) + c_{11} + \tilde{c}_{11} \ln\left(\frac{M^2}{\hat{s}}\right) + \tilde{\tilde{c}}_{11} \ln\left(\frac{M_F^2}{\hat{s}}\right) + c_{12}\frac{\ln(1-v+vw)}{1-w} + c_{13}\frac{\ln w}{1-w} + c_{14}\frac{\ln\left(\frac{1-v}{1-vw}\right)}{1-w} \ , \end{aligned} \tag{21}$$

and expressions are given for the coefficients c_i. The FORTRAN code for these coefficients can be obtained upon request [37]. We note here that the coefficients obtained for the direct processes [Eq. (18)] are of identical form to the corresponding ones for the once-resolved processes involving a gluon in the initial state [the third and fourth processes in Eq. (20)] once terms proportional to N_C are eliminated. Since the matrix elements were integrated separately, this serves as a check on both calculations.

A detailed comparison with the results published in Ref. [15] for the direct processes [Eq. (18)] and those contained in the FORTRAN code of Ref. [14] for the once-resolved processes [Eq. (20)] revealed only (numerically insignificant) differences traceable to the different conventions for the spin averaging of the incoming photons and gluons mentioned above. Since the results for the direct processes can be obtained directly from Ref. [15] in a similar form to those in Appendix A, we display these for completeness only. In the case of the once-resolved processes, the results in Appendix B cannot, except for the coefficients multiplied by $\delta(1-w)$ and the "plus" distributions, be directly compared with those in the FORTRAN code of Ref. [14], since they are cast in a slightly different format. Any comparison has to be made before the results are cast in the form given in Eq. (21). Note that there is also a superfluous factor of 2 present in the coefficients of both Refs. [14] and [15], which is later canceled out when the cross section is calculated.

The contributions from the twice-resolved processes are exactly those relevant for hadron-hadron scattering, and all higher corrections to these have been calculated [16] and the results are generally available. We make use of these matrix elements in our calculation.

Finally, a note on the use of the coefficients in a numerical calculation. If, as in Eqs. (1) and (5), the lower limit of the w integration is not zero, but has a value A, then the "plus" distributions must be transformed via

$$\frac{1}{(1-w)_+} \to \frac{1}{(1-w)_A} + \ln(1-A)\delta(1-w) ,$$

$$\left(\frac{\ln(1-w)}{1-w}\right)_+ \to \left(\frac{\ln(1-w)}{1-w}\right)_A + \frac{1}{2}\ln^2(1-A)\delta(1-w) , \tag{22}$$

where the new distributions are defined by

$$\int_A^1 \frac{f(w)}{(1-w)_A}dw = \int_A^1 \frac{f(w)-f(1)}{(1-w)}dw \tag{23}$$

and similarly for $\{\ln(1-w)/(1-w)\}_+$. Also, when the reversed processes, i.e., $x_1 \leftrightarrow x_2$, are required, for example, $q\gamma \to q + X$, then the replacements

$$v \to 1-vw, \quad w \to \frac{1-v}{1-vw} \tag{24}$$

are necessary.

IV. NUMERICAL RESULTS

In this section we present numerical results for π^0 photoproduction first at e^+e^- colliders (LEP 2) and then at the ep collider HERA. In both calculations we use the Glück-Reya-Vogt (GRV) [21] and Gordon-Storrow (GS) [22] parametrizations of the photon distributions which are available both in LO and NLO, and we use exclusively the GRV proton distributions after checking that the Martin-Roberts-Stirling set D'_ [MRS(D'_)] [38] give very similar results. We shall see that the GRV and GS distributions represent steep and flat distributions, respectively, in the low-x region and between them should bracket the extremes of reasonable estimates for these functions. For the π^0 fragmentation functions, we use the recent NLO parametrizations of Ref. [19] which are in the $\overline{\text{MS}}$ scheme and take set I as standard after checking that set II gives essentially similar results. There are no corresponding LO sets for these distributions.

Throughout this calculation we try to be consistent by using only LO parameters in LO estimates of the cross section and NLO parameters in NLO estimates. By NLO we mean the full cross section of LO contributions plus higher-order corrections as implied in Eqs. (1) and (5). Thus, for example, when evaluating K factors the denominators are evaluated using LO hard subprocess sections with LO evolved parton distributions as well as the LO expression [Eq. (8)] for the strong coupling. The only exceptions to this are, of course, the fragmention functions. We use the approximation

$$\alpha_s(\mu^2) = \frac{2\pi}{\beta_0 \ln(\mu^2/\Lambda^2)}\left[1 - \frac{\beta_1 \ln[\ln(\mu^2/\Lambda^2)]}{\beta_0^2 \ln(\mu^2/\Lambda^2)}\right] \tag{25}$$

for the strong coupling, where $\beta_1 = 102-38/3N_f$, and N_f the number of active quark flavors is fixed to 4. The value of the QCD scale parameter Λ is chosen to correspond to the photon distributions in use, except at HERA, where we always choose it to correspond with the proton distributions. Finally, unless otherwise stated, the scales $\mu^2 = M^2 = M_F^2 = p_T^2$ are always used.

A. π^0 production at LEP 2

At LEP 2 we take the energy in e^+e^- center-of-mass system (c.m.s.) to be fixed at $\sqrt{S_{e^+e^-}} = 200$ GeV. This corresponds to a 100 GeV electron and/or positron beam energy in Eq. (2).

In Fig. 4 we show the K factor for the full cross section, i.e., the sum of direct and once- and twice-resolved contributions, defined by

$$K = \frac{\left(\frac{d\sigma}{dp_T dy}\right)_{\text{NLO}}}{\left(\frac{d\sigma}{dp_T dy}\right)_{\text{LO}}} \tag{26}$$

at rapidity $y = 0$ for the produced π^0, as given by the GS

and GRV distributions, as a function of p_T. This quantity is usually taken to indicate the relative importance of the higher-order corrections to a process and thus to determine the good behavior of the perturbation series if it is reasonably small, i.e., less than about 1.5 (when the corrections are positive). Clearly, the K factor is within this region for both distributions, but shows the expected rise at the extremes of phase space. The GRV distributions give consistently larger K factors, but the two diverge significantly only in the low-x_T ($x_T = 2p_T/\sqrt{S} \leq 0.1$) region. The explanation for this behavior is not clear since the LO and NLO versions of both sets of distributions were consistently used.

We next compare in Fig. 5 the various contributions to the cross section in NLO at $y = 0$ using the GS distributions. As expected, the contributions involving the photon distributions are significant in the lower-p_T (≤ 5 GeV) region only when compared to the direct contribution. Sensitivity of the cross section to these functions can therefore only be expected in this region. In addition, the cross section is small outside the lower-p_T region and thus may not be easily measurable. When the GRV distributions are used instead, both the once- and twice-resolved contributions are increased relative to the direct. As can be seen from Fig. 6, the full cross section is increased by as much as 45% relative to the GS prediction. This reflects the larger gluon distribution of the GRV parametrization, which, of course, also leads to larger quark distributions in the low-x region.

Making the reasonable assumption that only the full (the sum of the three contributions) cross section will yield enough events to be of use for constraining the QCD parameters, we show in Figs. 7(a) and 7(b) the p_T distributions for the full cross section using the GS and GRV parametrizations, respectively. The dashed curves show the effect of neglecting completely the contributions for gluons in the initial state, i.e., setting $g^\gamma = 0$. Short of evolving new distributions with different inputs for the gluon, this is perhaps the best way of checking sensitivity to g^γ. We see, as expected, that sensitivity to g^γ is restricted to the low-p_T region only. The magnitude of this sensitivity can be seen more clearly in Figs. 8(a) and 8(b), where we show the rapidity distributions at for

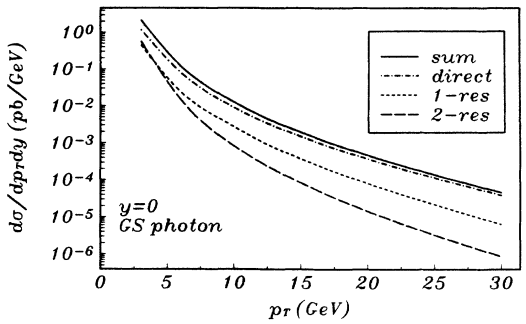

FIG. 5. p_T distributions for the various contributions to the inclusive π^0 cross section at LEP 2 and their sum, as predicted by the GS photon distributions.

$p_T = 5$ GeV. Clearly, measurement with good statistics would be able to discriminate between the two curves in each case and thereby determine the presence of a contribution from g^γ. Such measurements may quite possibly also be able to discriminate between the GS and GRV distributions, since, as can be easily seen, they give different predictions for the cross section.

To be certain of measuring g^γ, it would, of course, be better to increase the c.m.s. energy in the e^+e^- system. Figure 9 shows the p_T distributions for all three contributions and their sum at $y = 0$ using the GRV distributions for a c.m.s. energy of $\sqrt{S_{e^+e^-}} = 1000$ GeV. The cross section is obviously significantly larger than at LEP 2, and furthermore the double-resolved contributions will dominate the cross section for $p_T \leq 10$ GeV. The single-resolved contribution, which of course is also sensitive to the photon distributions, is also increased relative to the direct one in this p_T region.

To summarize, measurement of the cross section of single inclusive π^0 photoproduction at LEP 2 could yield as much information on the photon distribution functions as the study of jet production at TRISTAN has [1], and if in the future the c.m.s. energy could be increased at e^+e^- colliders, then there is no doubt that π^0 photoproduction will yield quantitative information on these functions and perhaps other QCD parameters.

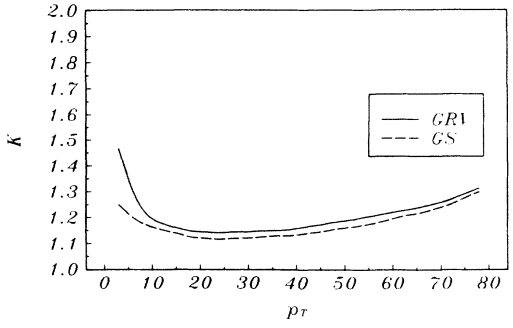

FIG. 4. K factor as defined in the text for the full inclusive cross section for π^0 production at LEP 2 at $y = 0$, as given by the GRV (solid line) and GS (dashed lines) parametrizations of the photon distributions.

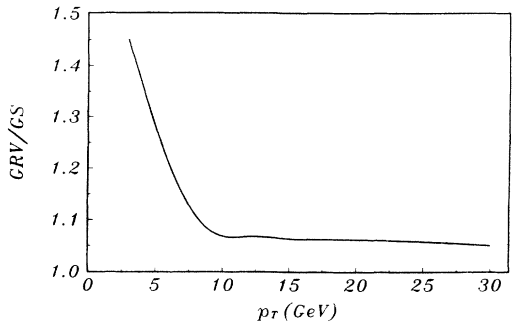

FIG. 6. Ratio of the GRV to the GS predictions for the full (sum) cross section given in Fig. 5.

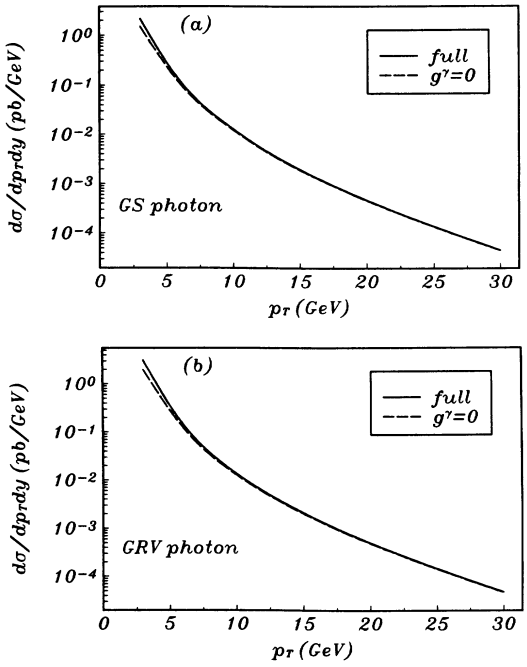

FIG. 7. Full inclusive π^0 cross section at LEP 2 at $y = 0$ with (solid lines) and without (dashed lines) gluon-initiated processes included for (a) the GS and (b) the GRV parametrizations of the photon distributions.

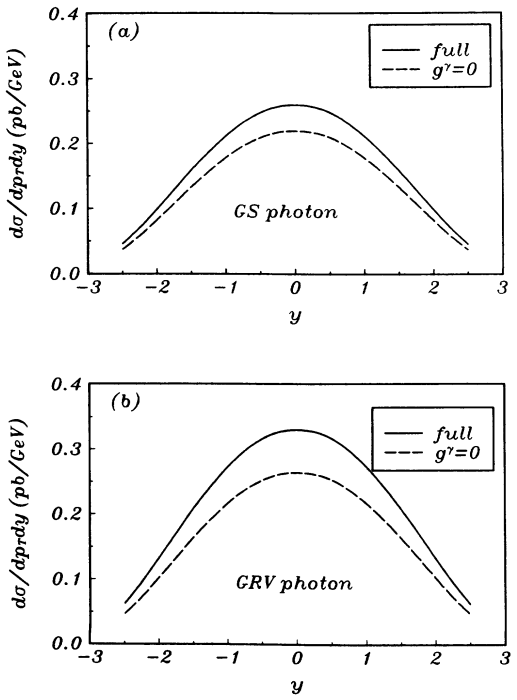

FIG. 8. Same as Fig. 7, but for rapidity distributions at $p_T = 5$ GeV.

B. π^0 production at HERA

The ep collider HERA offers at the present time the best opportunity for the study of photoproduction processes. The large c.m.s. energy $\sqrt{S_{ep}} \sim 300$ GeV means that an extended kinematic region may be probed as compared to the situation at e^+e^- machines. As far as measurement of the photon distribution functions are concerned, a possible drawback with a γp as opposed to a $\gamma\gamma$ reaction is that it must be assumed that the proton distributions are known. For example, in processes initiated by gg scattering, if g^p is not known, then one extra unknown is present as compared to the case of initial $g^\gamma g^\gamma$ scattering. Luckily, the parton distributions of the proton are presently far more accurately known than those for the photon, thus largely removing this potential handicap.

In our numerical study we present results exclusively for the GRV [20] proton distributions and fix the electron and proton beam energies at 30 and 820 GeV, respectively. Negative rapidity is taken as the direction in which the proton is traveling. As we shall see, this last choice results in a boosting of the reaction products toward negative rapidity as a result of the significantly larger proton beam energy. In this region the photon distributions are probed at smaller x, which can be a positive feature since this is precisely the region where they are least accurately known. The exploitation of this asymmetry in the rapidity distribution of the cross section is of course restricted by detector design limitations, which restricts the region where the cross section can be measured to $y \geq -2$ to -3. It will nevertheless still aid in mesauring the photon distributions since, as we shall see, it means that the direct contributions will be suppressed relative to the resolved ones at negative rapidity in the low- to medium-p_T region where the cross section will be largest. The explanation for this effect is quite simply that the direct contributions involve a reaction with a more energetic particle (the photon) moving toward positive rapidity than do the resolved contributions, where the photon must first produce a parton with only some fraction of its own momentum, which then reacts with the proton. Thus, as we shall see, tagging of the photon fragments with all its attendant difficulties in order to identify the resolved contributions will prove unnecessary in certain interesting kinematic regions.

Figure 10 shows the rapidity distribution of the resolved and direct contributions both in LO and NLO at $p_T = 5$ GeV for the GRV and GS distributions. The first obvious feature of the results is that the higher-order corrections to both contributions are relatively small in all the regions displayed (the GRV LO and NLO curves for the resolved contributions must be compared). Thus the perturbation stability of the predictions is immediately established. It is also very clear that the GRV and GS photon distributions give significantly different predictions for the resolved contributions, indicating that the cross section is sensitive to the photon distributions in this region. Finally, as we anticipated above, the resolved contributions totally dominate the cross section except in the very extreme positive rapidity region shown.

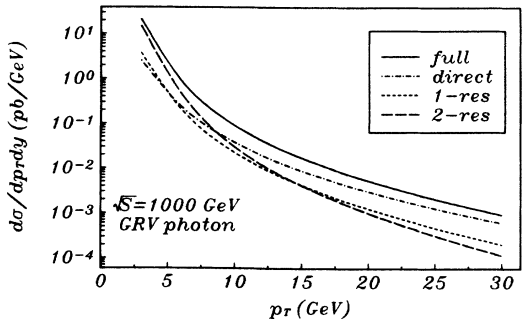

FIG. 9. p_T distributions for the various contributions to the inclusive π^0 cross section and their sum at an e^+e^- machine with c.m.s. energy $\sqrt{S_{e^+e^-}} = 1000$ GeV at rapidity $y = 0$ as predicted by the GRV photon distributions.

In Fig. 11 we see that the cross section is quite substantial out to $p_T \sim 25$ GeV at $y = -2$, and thus there should be many events accumulated here in the experiments. It can also be seen that the resolved contributions still dominate the cross section out to this p_T value, as predicted by both the GRV and GS distributions. This is seen even more clearly in Fig. 12, where we plot the ratio of direct to resolved contributions vs p_T at the same rapidity for both parametrizations of the photon distributions. Here the difference between the GS and GRV predictions show up even more clearly. According to GRV, the direct contributions do not overtake the resolved until $p_T \sim 40$ GeV, whereas for GS the value is about 30 GeV.

In order to check for sensitivity to the photonic gluon g^γ, we show in Figs. 13(a) and 13(b), for the GS and GRV parametrizations, respectively, the effect on the resolved contributions of neglecting all gluon-initiated processes by setting $g^\gamma = 0$ in the calculation. In both cases the effect is a very significant fall in the predicted cross section which is most significant, as may be expected, in the low-p_T region. For the GS distributions at $p_T = 5$ GeV, there is a 55% fall in the cross section, while at $p_T \sim 40$ GeV the reduction is only $\sim 13\%$. The corresponding figures for GRV are 50% and 10%, respectively. We can safely conclude from these figures that the cross section is quite sensitive to g^γ in the lower-p_T region

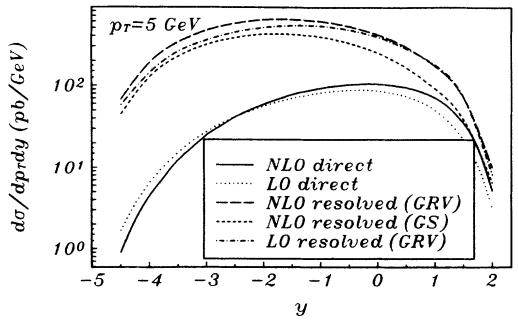

FIG. 10. Rapidity distributions at $p_T = 5$ GeV for resolved and direct contributions to the inclusive π^0 differential cross section at HERA in LO and NLO. For the GRV photon and LO resolved contribution is included, while for the GS photon only the NLO prediction is included.

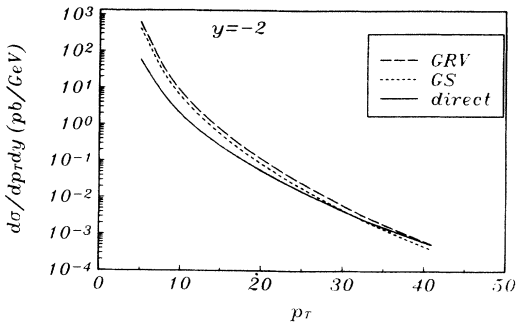

FIG. 11. p_T distributions for the resolved and direct contributions to the inclusive π^0 cross section at HERA in NLO at $y = -2$. In the case of the resolved contributions, results are shown for the GS (short dashed lines) and GRV (long dashed lines) photon distributions.

around $y = -2$.

Figure 14 shows the scale dependence of the cross section (in NLO) at $p_T = 10$ GeV. Included for comparison are the separate scale dependences of the resolved and direct contributions. In Fig. 14(a) we vary all the scales in the cross section; i.e., we set $\mu = M = M_F = \xi p_T$ and vary ξ in the region $0.2 \leq \xi \leq 2$. It is quite obvious that the direct and particularly the resolved contributions separately have very significant dependences on the scales, but as can be seen adding the two together significantly reduces this dependence. If we measure the scale dependence by the ratio of the maximum to the minimum value of the cross section obtained by varying ξ between the limits stated above, then the direct and resolved contributions have scale dependences of magnitude 6 and 12.6, respectively, whereas the sum has a dependence of just 2.

Figure 14(b) shows the effect of varying the factorization scale M only while holding the other scales fixed at $\mu = M_F = p_T$. This demonstrates nicely the operation of the scale compensation mechanism discussed in Sec. II B. The direct and resolved contributions have separately scale dependences of magnitudes 3.2 and 1.4, respectively, while the sum has a value of less than 1.1, as depicted by the almost flat line in the figure.

Finally, in Fig. 15 we compare the scale dependence of

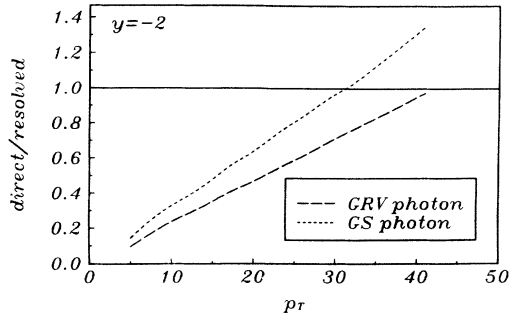

FIG. 12. Ratio of direct to resolved contributions to the cross sections as shown in Fig. 11.

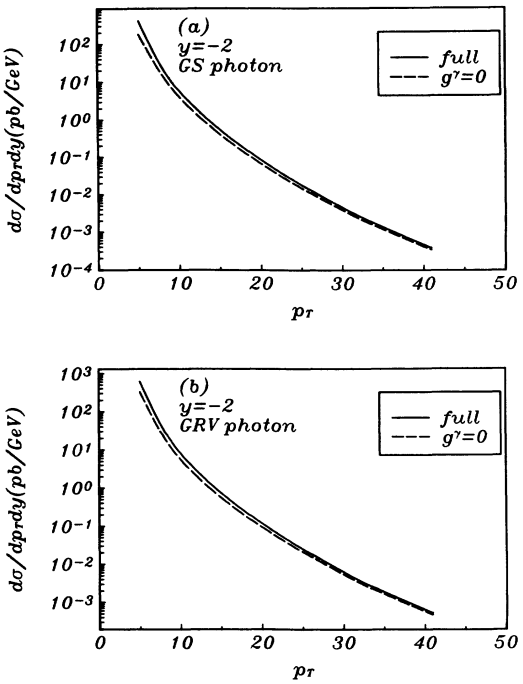

FIG. 13. p_T distributions for the resolved contributions to the inclusive π^0 cross section at HERA in NLO at $y = -2$ with (solid lines) and without (dashed lines) contributions from processes initiated by a gluon from the photon included for (a) the GS and (b) the GRV photon distributions.

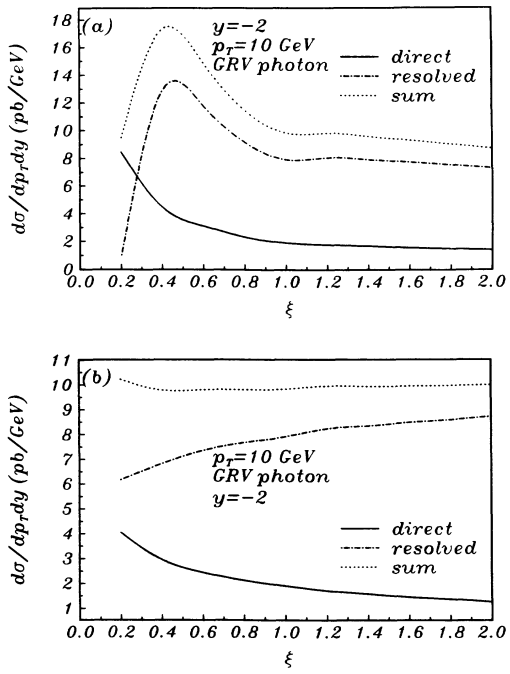

FIG. 14. (a) Scale dependence of the inclusive π^0 cross section at HERA in NLO at $p_T = 10$ GeV and $y = -2$, showing the separate scale dependences of the direct and the resolved contributions and that of the sum. All scales are varied in (a). (b) same as (a), but where only the factorization scale M^2 is varied.

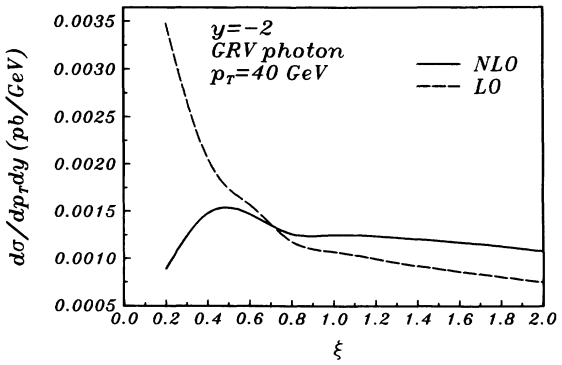

FIG. 15. Comparison of the scale dependence of the full inclusive π^0 differential cross section at $p_T = 40$ GeV and $y = -2$ at HERA as given in LO (dashed line) and NLO (solid line).

the full LO and NLO predictions for the cross section at $p_T = 40$ GeV, where all scales are varied. As one would expect, the NLO prediction has a much weaker scale dependence than the LO one. The magnitudes, as defined above, are 4.6 for the LO and 1.6 for the NLO prediction. We also see, as demonstrated in many places before, that the LO and NLO predictions coincide at around $\xi \sim 1$, indicating that the usual choice of scales corresponding to this value for ξ lead to maximum perturbative stability for the predictions.

C. Comparison with existing data

Recently, the Mark II Collaboration at the SLAC e^+e^- storage ring PEP has published single tagged data for inclusive charged hadron production at $\sqrt{S} = 29$ GeV [8]. A comparison with the theoretical predictions of Aurenche *et al.* [15] has shown a significant discrepancy between theory and data at larger p_T (≥ 1.5 GeV). In the calculation of Ref. [15], the twice-resolved contributions were estimated in LO only, and simple vector meson dominance (VMD) estimates for the photon distributions were used throughout. Furthermore, the old LO parametrizations for the $\pi^{\pm}$ and $K^{\pm}$ fragmentation functions [39] were used. Although the value of $\sqrt{S} = 29$ GeV is rather low and the data were collected at low p_T, making the application of a perturbative calculation questionable to some, it is still interesting to see whether a full NLO treatment using modern photon distributions and fragmentation functions [40] will provide any improvement in the agreement between theory and experiment.

In Fig. 16 we make a comparison with the Mark II data using the GRV photon distributions. It is very clear that although the NLO predictions show a marginal improvement over the LO ones, this is not sufficient to explain the data. We also show in Fig. 16, for comparison, contributions from the direct once- and twice-resolved processes. It is obvious that above about $p_T \geq 2$ GeV, the direct contribution is very much the dominant one. This means that, except for the fragmentation functions, there are no significant nonperturbative inputs in the prediction.

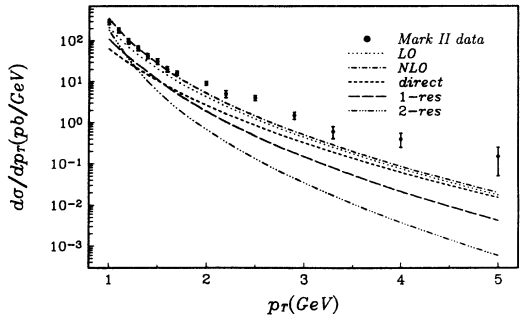

FIG. 16. Comparison of the LO and NLO predictions using the GRV photon distributions and the new charged hadron fragmentation functions of Ref. [40] with the Mark II data.

In order to test the effect of the fragmentation functions, which are probed at $z \geq 0.15$ above $p_T \geq 2$ GeV, we froze these functions at $Q^2 = 2$ GeV^2. The effect is an increase of 20–30 % above $p_T = 2$ GeV, which is still far from sufficient to fit the data in this region. The only way to fit these data would be to radically increase the fragmentation functions in this region, but the freedom to do this is not available since they are somewhat constrained by other data [39,40]. The explanation for the discrepancy is thus not clear, but in Ref. [8] the idea was advanced that the excess of events above $p_T \geq 1.5$ GeV may be partly due to multijet processes not taken into account in the theoretical calculations. It will be very interesting to see whether similar measurements at LEP 1 and LEP 2, where much higher c.m.s. energies are available, will improve the situation.

V. CONCLUSIONS

We have performed the first complete and consistent calculation of inclusive hadron photoproduction at e^+e^- and ep machines in NLO QCD. Our predictions show the expected reduced sensitivity to variations in the factorization and/or renormalization scales over the corresponding LO ones, although for reasonable choice of scales the sizes of the higher-order corrections are still quite small, indicating the perturbative stability of the cross sections. These results highlight the by now well-known fact that beyond LO calculations have the potential to allow for quantitative tests of QCD theory, provided that important parameters such as structure and fragmentation functions are accurately known.

The results of our study of inclusive π^0 production at LEP 2 and HERA indicate sensitivity to the photon distributions in kinematic regions which are accessible for measurements. This means that measurement of the cross sections will yield useful information on these functions. We have also shown that increasing the c.m.s. energy in the e^+e^- system to 1000 GeV would significantly enhance the cross section, leading to easier measurement of the cross section as well as to increased sensitivity to the photon distributions.

A comparison of the theoretical predictions with the single tagged Mark II data on inclusive charged hadron production fails to remove the discrepancy above $p_T \geq 1.5$ GeV.

ACKNOWLEDGMENTS

I thank W. Vogelsang for many helpful discussions and for carefully reading the manuscript. I would also like to thank J. K. Storrow for reading the manuscript. I am also grateful to J.-Ph. Guillet for providing me with the FORTRAN code for the double-resolved and/or once-resolved processes and to M. Fontannaz for giving me permission to compare with the matrix elements of Ref. [14] and to B. A. Kniehl for supplying them.

APPENDIX A: THE PROCESSES $\gamma\gamma \to c + X$

We list here our results for the integrated matrix elements for inclusive production of quarks and gluons from photon-photon collisions. We make use of the abbreviations

$$Y = 1 - v + vw\ , \quad X = 1 - vw\ ,$$
$$v_i = i - v\ , \quad T_{\gamma\gamma} = \left(\frac{v}{1-v} + \frac{1-v}{v}\right)\ ,$$

where $i = 1, 2, 3$. $\lambda = 1$ should be taken as discussed in Sec. III. The LO Born cross section $\gamma\gamma \to q\bar{q}$ is

$$\frac{d\hat{\sigma}}{dv} = \frac{2\pi\alpha_{\rm em}^2 N_C e_q^4}{\hat{s}} T_{\gamma\gamma}\ .$$

1. $\gamma\gamma \to q(\bar{q}) + X$

$$\tilde{c}_1 = 0, \quad \hat{c}_1 = 0, \quad \tilde{c}_2 = 0\ ,$$
$$c_1 = \frac{C_F N_C T_{\gamma\gamma}}{1 - 2vv_1}\left[\ln v_1 v(2+v) - \frac{\ln v(-3+2v+4v^2)}{2} + \ln^2 v(3v^2+2v_1)\right.$$
$$\left. + \left(-\frac{7}{2} + \frac{2\pi^2}{3}\right)(1-2vv_1) + \ln^2 v_1(1+v_1^2)\right]\ ,$$

$$\tilde{\tilde{c}}_1 = \frac{-C_F N_C T_{\gamma\gamma}(3+4\ln v)}{2} ,$$
$$c_2 = \frac{C_F N_C T_{\gamma\gamma}(-3+4\ln v)}{2} ,$$
$$\tilde{\tilde{c}}_2 = -2C_F N_C T_{\gamma\gamma} ,$$
$$c_3 = 2C_F N_C T_{\gamma\gamma} ,$$
$$c_5 = \frac{C_F N_C}{v v_1}\left(\frac{-2v^2 v_1}{X^2} - \frac{2v^2 v_1}{Y} - 2(1+2v^2)v_1 + \frac{2v^2 v_1^2}{X^3} + \frac{v^2(3-2vv_2)}{X} + \frac{v_1(3-2vv_1)}{w} - 2(-v^2+2v^3-v_1)w\right) ,$$
$$c_6 = C_F N_C\left(\frac{-2v^2(2-w)}{v_1} - \frac{2(1-2v)(v^2+v_2)}{v v_1 w}\right) ,$$
$$c_7 = \frac{-2C_F N_C}{Yvw}(Y+2v^2 w) ,$$
$$c_8 = \frac{2C_F N_C}{vw}(2-2v+v^2) ,$$
$$c_9 = \frac{-2C_F N_C}{v v_1 w}(-v_1+v^2 w+v^3 w^2) ,$$
$$c_{10} = c_5 - \frac{2C_F N_C}{v_1 w}[1+v^2(1-w)^2] ,$$
$$c_{11} = \frac{C_F N_C}{v v_1}\left(5 - \frac{v^2(-1-3v+v^2)}{X} + \frac{5v^2 v_1}{X^2} + \frac{2v^2 v_1}{Y} - \frac{6v^2 v_1^2}{X^3} - 3vv_2 + \frac{(3-2v+6v^2)v_1}{2w} - (v^2+2v^3+6v_1)w\right)$$
$$+\lambda\frac{C_F N_C}{v v_1}\left((3v^2-4v^3+2v_1) + \frac{2v^2 v_1}{X^2} - \frac{2v^2 v_1^2}{X^3} - \frac{v^2(3-2vv_2)}{X} - \frac{(1+v^2)v_1}{w} - (2v^2-3v^3+2v_1)w\right) ,$$
$$\tilde{c}_{11} = C_F N_C\left(\frac{2v}{X^2} - \frac{-3v^2+4v^3-2v_1}{v v_1} - \frac{2vv_1}{X^3} - \frac{v(3-2vv_2)}{X v_1} - \frac{(1+v^2)}{vw} + \frac{(-2v^2+3v^3-2v_1)w}{v v_1}\right) ,$$
$$\tilde{\tilde{c}}_{11} = C_F N_C\left(\frac{2v}{Y} + \frac{v}{v_1} - \frac{1+v_1^2}{vw} + \frac{v^2 w}{v_1}\right) ,$$
$$c_{12} = \frac{-2C_F N_C}{v_1 v}(1+2vv_1) ,$$
$$c_{13} = \frac{2C_F N_C}{v v_1}(1+v^2) ,$$
$$c_{14} = \frac{2C_F N_C}{v v_1}(1+v_1^2) .$$

2. $\gamma\gamma \to g + X$

$$c_1 = 0,\ \tilde{c}_1 = 0,\ \tilde{\tilde{c}}_1 = 0,\ \hat{c}_1 = 0,\ c_2 = 0,\ \tilde{c}_2 = 0,\ \tilde{\tilde{c}}_2 = 0,\ c_3 = 0 ,$$
$$c_{12} = 0,\ c_{13} = 0,\ c_{14} = 0 ,$$
$$c_5 = 8C_F N_C\left(-\frac{v}{Y^2} + \frac{v v_1}{X^2} - \frac{v^2+v_1}{v_1} - \frac{v^2}{Y v_1 v_2} - \frac{v^2 v_1}{X v_2} + \frac{2v^2+v_1}{v_1 w} + \frac{(v^2+v_1)w}{v_1}\right) ,$$
$$c_6 = C_F N_C\frac{-4(Y^2+v^2)}{v_1 w} ,$$
$$c_7 = \frac{-16C_F N_C}{Y^2}[v^2(1-w)] ,$$
$$c_8 = C_F N_C\left(\frac{-8(1+v_1^2)}{X v_2} + \frac{8(1+v_1^2)}{Y v_1 v_2} - \frac{8v(1-w)}{v_1} + \frac{4v_1}{w}\right) ,$$
$$c_9 = \frac{4C_F N_C}{v_1}\left(2v_1 - \frac{2(1+v_1^2)}{Y v_2} - \frac{2v_1^2(1+v_1^2)}{X v_2} + \frac{2(v^2+v_1)}{w} + v^2 w\right) ,$$

$$c_{10} = c_5 + \frac{4C_F N_C}{v_1}\left(-2(1-vv_1) + \frac{2(1+v_1^2)}{Yv_2} + \frac{2v_1^2(1+v_1^2)}{Xv_2} - \frac{v^2}{w} + v^2 w\right) ,$$

$$c_{11} = \frac{4C_F N_C}{v_1 w}(1+v_1^2+v^2w^2) + \lambda\frac{2C_F N_C}{v_1}\left(2(2-3v+2v^2) + \frac{4vv_1}{X} - \frac{4vv_1^2}{X^2} - \frac{3-4v+3v^2}{w} - (3v^2+4v_1)w\right) ,$$

$$\tilde{c}_{11} = \frac{2C_F N_C}{v_1}\left(2(2-3v+2v^2) + \frac{4vv_1}{X} - \frac{4vv_1^2}{X^2} - \frac{3-4v+3v^2}{w} - (3v^2+4v_1)w\right) ,$$

$$\tilde{\tilde{c}}_{11} = \frac{-2C_F N_C}{Y^2 v_1 w}[1+v^2(1-w)^2](v_1^2+v^2w^2) .$$

APPENDIX B: THE PROCESSES $\gamma b \to c + X$

Here we list the results for the case of one pointlike photon coupling in the initial state. For convenience we give the contributions for the inclusive process $\gamma q \to q + X$ in three parts which we label (a), (b), and (c). These contributions should be added to give the full cross section for the subprocess, but note that (c) is the part proportional to $e_q'^2$ derived from the process $\gamma q \to q\bar{q}'q'$ (where q is the observed particle). The part proportional to e_q^2, which also contains distributions, has been absorbed into part (a). A similar modification of part (b) was also done. In addition to being more convenient for programming purposes, this procedure also leads to a further shortening of the matrix elements.

The abbreviations X, Y, and v_i are already defined in Appendix A.

The relevant $2 \to 2$ Born cross sections are, for $\gamma q \to qg$,

$$\frac{d\hat{\sigma}}{dv} = \frac{2\pi\alpha_s\alpha_{\rm em}e_q^2}{\hat{s}} C_F T_{\gamma q}^{(1)} ,$$

for $\gamma q \to gq$,

$$\frac{d\hat{\sigma}}{dv} = \frac{2\pi\alpha_s\alpha_{\rm em}e_q^2}{\hat{s}} C_F T_{\gamma q}^{(2)} ,$$

and for $\gamma g \to q\bar{q}$,

$$\frac{d\hat{\sigma}}{dv} = \frac{\pi\alpha_s\alpha_{\rm em}e_q^2}{\hat{s}} T_{\gamma g} ,$$

where

$$T_{\gamma q}^{(1)} = \frac{1+(1-v)^2}{(1-v)} ,$$

$$T_{\gamma q}^{(2)} = \frac{1+v^2}{v} ,$$

$$T_{\gamma g} = \frac{1-v}{v} + \frac{v}{1-v} .$$

We also define the constant

$$b_0 = \tfrac{11}{6}N_C - \tfrac{1}{3}N_F .$$

1. $\gamma q \to q + X$ [part (a)]

$$c_1 = \frac{C_F T_{\gamma q}^{(1)}}{1+v_1^2}\left[C_F \ln(v_1)(1+2v) + \left(C_F - \frac{N_C}{2}\right)\ln^2(v_1)(3-4v+3v^2) - (2C_F - N_C)\ln(v_1)\ln(v)(7-8v+5v^2)\right.$$
$$-\frac{N_C\pi^2}{6}(1-4v+5v^2) + N_C\ln(v_1)v_1 + 2(2C_F - N_C)\ln(v)v_1 - \frac{N_C\ln^2(v)}{2}(9v^2+14v_1) + C_F\ln^2(v)$$
$$\left.\times(11v^2+18v_1) + C_F\pi^2(1-2vv_1) - \left(7C_F - \frac{2N_C}{3}\right)(1+v_1^2) + \frac{5b_0}{3}(1+v_1^2) - b_0\ln(v)(1+v_1^2)\right] ,$$

$$\tilde{c}_1 = \frac{C_F^2 T_{\gamma q}^{(1)}}{2}[-3 + 4\ln(v_1) - 4\ln(v)] ,$$

$$\tilde{\tilde{c}}_1 = -\frac{C_F^2 T_{\gamma q}^{(1)}}{2}[3 + 4\ln(v)] ,$$

$$\hat{c}_1 = C_F T_{\gamma q}^{(1)} b_0 ,$$

$$c_2 = [-C_F b_0 - 2C_F(2C_F - N_C)\ln(v_1) + 4C_F(3C_F - N_C)\ln(v)]T_{\gamma q}^{(1)} ,$$

$$\tilde{c}_2 = -2C_F^2 T_{\gamma q}^{(1)} ,$$

$$\tilde{\tilde{c}}_2 = -2C_F^2 T_{\gamma q}^{(1)} ,$$

$$c_3 = 2C_F(4C_F - N_C)T_{\gamma q}^{(1)} ,$$

$$c_5 = C_F^2\left(-\frac{v}{X^2} + \frac{vv_1}{Y^2} + \frac{v(10 - 11v + 5v^2)}{Yv_2} - \frac{v(10 - 9v + 4v^2)}{Xv_1v_2} - \frac{10v^2w}{v_1}\right) + \frac{C_F N_C}{XYv_1}(2v^2v_2^2w + 4v^4w^2 - 4v^4w^3) ,$$

$$c_6 = \frac{2C_F}{v_1}(2C_F - N_C)v^2w ,$$

$$c_7 = \frac{-2C_F N_C v^2 w}{v_1} + \frac{2C_F^2 v^2 w}{Y^2 v_1}[-2v_1 - v^2(1 - w)w] ,$$

$$c_8 = \frac{C_F}{XY}(2C_F - N_C)T_{\gamma q}^{(1)} v^2 w ,$$

$$c_9 = \frac{C_F(2C_F - N_C)v^2w}{XYv_1}(-v^2 - 4v_1 - 2v^2w + 2v^2w^2) ,$$

$$c_{10} = C_F^2\left(-\frac{v}{X^2} + \frac{vv_1}{Y^2} + \frac{v(6 - 7v + 3v^2)}{Yv_2} - \frac{v(6 - 5v + 2v^2)}{Xv_1v_2} - \frac{6v^2w}{v_1}\right) - \frac{C_F N_C v^2 w}{XYv_1}(-v^2 - 4v_1 - 2v^2w + 2v^2w^2) ,$$

$$c_{11} = \frac{C_F^2 v^2}{v_1}\left(2 + \frac{v_1}{X^2 v} - \frac{3v_1}{Xv} + \frac{3v_1}{Yv} - \frac{v_1^2}{Y^2 v}\right) + \frac{2C_F b_0 v^2 w}{v_1}$$
$$-\frac{C_F N_C v^2 w}{2X^2Y^2v_1}(1 + v_1^2 - 2v^2w + 2v^2w^2)(-4v_1 - 3v^2w + 3v^2w^2) ,$$

$$\tilde{c}_{11} = \frac{C_F^2 v^2 w}{X^2 v_1}(-2 + vw)(-v_2 + vw) ,$$

$$\tilde{\tilde{c}}_{11} = \frac{C_F^2 v^2 w}{Y^2 v_1}(2v_1 + vw)(v_2 + vw) ,$$

$$c_{12} = C_F N_C T_{\gamma q}^{(1)} ,$$

$$c_{13} = 2C_F(2C_F - N_C)T_{\gamma q}^{(1)} ,$$

$$c_{14} = C_F(6C_F - N_C)T_{\gamma q}^{(1)} .$$

2. $\gamma q \to q + X$ [part (b)]

$$c_1 = 0, \quad \tilde{c}_1 = 0, \quad \tilde{\tilde{c}}_1 = 0, \quad \hat{c}_1 = 0, \quad c_2 = 0, \quad \hat{c}_2 = 0, \quad \tilde{\tilde{c}}_2 = 0, \quad c_3 = 0 ,$$

$$c_5 = C_F\left(\frac{v}{2X^2} - \frac{v(-3 + 2v)}{2Y} - \frac{2(2 - 6v + 8v^2 - 6v^3 + 7v^4 - 5v^5 + 2v^6)}{v^2v_1^2} - \frac{vv_1}{2Y^2} - \frac{vv_3}{2Xv_1}\right.$$
$$\left. + \frac{2 - 6v + 9v^2 - 8v^3 + 9v^4 - 6v^5 + 2v^6}{v^2v_1^2w} + \frac{2}{v^2v_1^2}(2 - 6v + 8v^2 - 6v^3 + 7v^4 - 5v^5 + 2v^6)w\right)$$
$$-\frac{C_F}{N_C v_1 w}(v^2 + 3v_1)(1 - 2w + 2w^2) ,$$

$$c_6 = \frac{C_F}{N_C v_1}\left(2vv_2 - \frac{v}{w} - 2v^2w\right) + \frac{C_F}{v_1^2}\left(v(2 + v + v^2) - \frac{1 + v^2}{w} - 2v^2(1 + v)w\right) ,$$

$$c_7 = C_F\left(-\frac{v(-3 + 2v)}{Y} - \frac{vv_1}{Y^2} - \frac{vv_2}{v_1} + \frac{2v^2w}{v_1}\right) - \frac{C_F}{N_C v_1 w}v(-v_1 + 2v_2w + 2vw^2) ,$$

$$c_8 = \frac{C_F}{N_C}\left(\frac{2vv_2}{v_1} + \frac{-2+3v-2v^2v_2}{vv_1w} - 4vw\right) + \frac{C_F}{v_1^2}\left(-2v(v^2+v_2) + \frac{1+v^2}{w} + 4v(v^2+v_1)w\right) ,$$

$$c_9 = \frac{C_F}{N_C v_1}\left(4(1-vv_1) - \frac{v^2+3v_1}{w} + 2v^2w\right) + C_F\left(-\frac{2-4v+15v^2-13v^3+4v^4}{v_1^2} + \frac{2(1-2v+4v^2-3v^2+v^4)}{v_1^2 w}\right.$$
$$\left. + \frac{2v^2(2v^2+7v_1)w}{v_1^2} - \frac{8v^2w^2}{v_1}\right) ,$$

$$c_{10} = c_5 - \frac{C_F}{N_C v_1 w}[3v_1 + 2v^2(1-w)^2 - 4v_1 w] - \frac{C_F}{v_1}(1+4v^2+v_1^2-10v^2w+8v^2w^2) ,$$

$$c_{11} = C_F\left(-\frac{v}{X^2} + \frac{2(6-18v+19v^2-8v^3+3v^4-2v^5+v^6)}{v^2v_1^2} + \frac{vv_1}{Y^2} - \frac{3vv_2}{2Y} + \frac{3vv_2}{2Xv_1}\right.$$
$$\left. + \frac{1}{w} - \frac{(12-36v+38v^2-16v^3+7v^4-5v^5+2v^6)w}{v^2v_1^2}\right)$$
$$+ \frac{C_F}{N_C}\left(-2 + \frac{v}{2X^2} - \frac{3v}{2Xv_1} - \frac{vv_1}{2Y^2} + \frac{3vv_1}{2Y} - \frac{v^2+3v_1}{v_1 w} + \frac{(3v^2+4v_1)w}{v_1}\right)$$
$$+ \lambda\left[\frac{C_F}{2v^2v_1}\left(\frac{v^3v_1}{X^2} - \frac{v^3v_3}{X} + 4(-2+v^5+4vv_1+2v^3v_1)(-1+w) - \frac{v_1(3v^2+4v_1-2v^3v_1)}{w}\right)\right.$$
$$\left. + \frac{C_F}{N_C v_1 w}(v^2+3v_1)(1-2w+2w^2)\right] ,$$

$$\tilde{c}_{11} = \frac{C_F}{2}\left(-\frac{v}{X^2} + \frac{4(2-6v+8v^2-6v^3+6v^4-3v^5+v^6)}{v^2v_1^2} + \frac{vv_3}{Xv_1} - \frac{4-12v+17v^2-12v^3+11v^4-6v^5+2v^6}{v^2v_1^2 w}\right.$$
$$\left. - \frac{4(2-6v+8v^2-6v^3+6v^4-3v^5+v^6)w}{v^2v_1^2}\right) + \frac{C_F}{N_C v_1 w}[(v^2+3v_1)(1-2w+2w^2)] ,$$

$$\tilde{\tilde{c}}_{11} = \frac{C_F}{2}\left(4v^2 + \frac{v(-3+2v)}{Y} + \frac{vv_1}{Y^2} - \frac{1-2vv_1}{w} - 4v^2w\right) ,$$

$$c_{12} = \frac{C_F}{N_C v_1}(1+v^2) ,$$

$$c_{13} = -\frac{C_F}{N_C v_1}(3v^2+2v_1) ,$$

$$c_{14} = -\frac{C_F}{N_C v_1}(1-2vv_1) .$$

3. $\gamma q \to q + X$ [part (c)]

$$c_1 = 0, \quad \tilde{c}_1 = 0, \quad \tilde{\tilde{c}}_1 = 0, \quad \hat{c}_1 = 0, \quad c_2 = 0, \quad \hat{c}_2 = 0, \quad \tilde{\tilde{c}}_2 = 0, \quad c_3 = 0 ,$$
$$c_7 = 0, \quad c_9 = 0, \quad \tilde{\tilde{c}}_{11} = 0, \quad c_{12} = 0, \quad c_{13} = 0, \quad c_{14} = 0 ,$$
$$c_5 = C_F e_q'^2 v \frac{[v_1^2 + v^2(1-w)^2](1+v^2w^2)}{X^4 v_1} ,$$
$$c_6 = -c_5 ,$$
$$c_8 = c_5 ,$$
$$c_{10} = c_5 ,$$
$$c_{11} = 2C_F e_q'^2 \frac{v^2(1-w)(1+4vw+v^2w^2)}{X^4} - \lambda c_5 ,$$
$$\tilde{c}_{11} = -c_5 .$$

4. $\gamma q \to g + X$

$$c_1 = \frac{C_F T_{\gamma q}^{(2)}}{1+v^2}\left[2(2C_F - N_C)\ln(v_1)v - \frac{7C_F}{2}(1+v^2) + \ln(v)\left(N_C v - \frac{C_F}{2}(-3+4v+3v^2)\right)\right.$$
$$+\ln^2(v_1)\left(2C_F v_1^2 - \frac{N_C}{2}(v_1^2-2v)\right) + \ln^2(v)\left(\frac{N_C}{2}(8+2v+7v^2) + C_F(3v^2+2v_1)\right)$$
$$\left. - \ln(v_1)\ln(v)[N_C(2+2v+v^2) + 2C_F(1-2vv_1)] + \pi^2\left(\frac{C_F}{3}(2-6v+5v^2) + \frac{N_C}{2}vv_2\right)\right] ,$$

$$\tilde{c}_1 = \frac{C_F^2 T_{\gamma q}^{(2)}}{2}[4\ln(v_1) - 4\ln(v) - 3] ,$$

$$\tilde{\tilde{c}}_1 = -C_F T_{\gamma q}^{(2)}[b_0 + 2N_c\ln(v)] ,$$

$$\hat{c}_1 = C_F T_{\gamma q}^{(2)} b_0 ,$$

$$c_2 = \left(-\frac{3C_F^2}{2} - 2C_F N_C\ln(v_1) + 2C_F(C_F+3N_C)\ln(v)\right)T_{\gamma q}^{(2)} ,$$

$$\tilde{c}_2 = -2C_F^2 T_{\gamma q}^{(2)} ,$$

$$\tilde{\tilde{c}}_2 = -2C_F N_C T_{\gamma q}^{(2)} ,$$

$$c_3 = 2C_F(C_F+2N_C)T_{\gamma q}^{(2)} ,$$

$$c_5 = C_F^2\left(\frac{-2v}{X} + \frac{2vv_1}{Y^3} - \frac{2vv_1}{Y^2} - \frac{2(2v^2+v_1^2)}{vv_1} + \frac{v(3-vv_2)}{Yv_1} + \frac{-3vv_1+v_3}{vv_1 w} + \frac{2(1+v^3-2vv_1)w}{vv_1}\right)$$
$$+C_F N_C\left(2(-1+2v)^2 - \frac{2v(6-7v+3v^2)}{Yv_1} - \frac{2vv_1}{Y^3} + \frac{2vv_2}{Y^2} + \frac{6-11v+15v^2-10v^3+4v^4}{vv_1 w} - 2(3v^2+v_1^2)w\right) ,$$

$$c_6 = \frac{C_F N_C}{vw}(v_1+v^2 w) + C_F^2\left(2v - \frac{2(3-2vv_2)}{vv_1 w} - \frac{2v^2 w}{v_1}\right) ,$$

$$c_7 = C_F^2\left(-2v + \frac{4vv_1}{Y^3} - \frac{4vv_1}{Y^2} + \frac{2v(3-vv_2)}{Yv_1} - \frac{2(1+v)}{vv_1 w}(2-3v+2v^2)\right)$$
$$+C_F N_C\left(7v - \frac{4v(4-5v+2v^2)}{Yv_1} - \frac{4vv_1}{Y^3} + \frac{4vv_2}{Y^2} + \frac{1+v}{vv_1 w}(3-4v+3v^2)\right) ,$$

$$c_8 = C_F N_C\left(\frac{2v(v^2+2v_1)}{Yv_1} - \frac{3+v^3-2vv_2)}{vv_1 w}\right) + C_F^2\left(\frac{-2v(1+v)}{v_1} + \frac{2(2v^3+3v_1)}{vv_1 w} + \frac{4v^2 w}{v_1}\right) ,$$

$$c_9 = C_F N_C\left(v(-5+8v) - \frac{2v(1+v_1^2)}{Yv_1} + \frac{(2-3v+2v^2)(2v^2+v_1)}{vv_1 w} - 8v^2 w\right) + \frac{2C_F^2}{vv_1 w}(v_1^2 - v^2 v_1 w + v^3 w^2) ,$$

$$c_{10} = c_5 + C_F N_C\left(v + \frac{2v(1+v_1^2)}{Yv_1} - \frac{1+v^3+v_1^2}{vv_1 w}\right) + \frac{2C_F^2}{v_1 w}[v_1^2 + v^2(1-w)^2] ,$$

$$c_{11} = C_F^2\left(\frac{2v}{X} + \frac{v(1-5v+3v^2)}{Yv_1} - \frac{6vv_1}{Y^3} + \frac{5vv_1}{Y^2} + \frac{5-2vv_2}{v} + \frac{3-4v+7v^2}{2vv_1 w} + \frac{(-6+12v-7v^2+3v^3)w}{vv_1}\right)$$
$$+C_F N_C\left(-2 - \frac{2v}{X} + \frac{v(-7+5v)}{Y^2} + \frac{6vv_1}{Y^3} + \frac{vv_3}{Y} - \frac{v^2+v_1^2}{w} + 2v_2 w\right)$$
$$-\lambda\frac{C_F}{vv_1 w}(1-2vv_1)(C_F - N_C vv_1)(1-2w+2w^2) ,$$

$$\tilde{c}_{11} = C_F^2\left(\frac{2v}{X} - \frac{-2+4v-5v^2+v^3}{vv_1} - \frac{3-4v+3v^2}{vv_1 w} - \frac{(2+v^3-4vv_1)w}{vv_1}\right) + \frac{C_F N_C}{w}(v^2+v_1^2)(1-2w+2w^2) ,$$

$$\tilde{\tilde{c}}_{11} = C_F N_C\left(-4v^2 + \frac{2v(4-5v+2v^2)}{Yv_1} + \frac{2vv_1}{Y^3} - \frac{2vv_2}{Y^2} - \frac{2(1-vv_1)^2}{vv_1 w} + 4v^2 w\right)$$

$$-\frac{C_F^2 v}{Y^3 v_1}[1+v^2(1-w)^2](2v_1^2+2vv_1w+v^2w^2)\ ,$$

$$c_{12}=C_F\left(\frac{N_C}{v}(3-2vv_1)-\frac{2C_F}{v}(1+v_1^2)\right)\ ,$$

$$c_{13}=C_F\left(\frac{N_C}{v}(2+2v+v^2)+\frac{2C_F}{v}(1-2vv_1)\right)\ ,$$

$$c_{14}=C_F\left(\frac{8C_F}{v}(1-vv_1)-\frac{N_C}{v}(-2v+v_1^2)\right)\ .$$

5. $\gamma g \to q + X$

$$c_1=\frac{T_{\gamma g}}{2(1-2vv_1)}\left[C_F\left(\frac{2\pi^2}{3}-\frac{7}{2}\right)(1-2vv_1)-4N_C\ln(v_1)\ln(v)(1-2vv_1)\right.$$
$$+\ln(v_1)[C_Fv(2+v)-N_CvV_1]+\ln(v)\left(-\frac{C_F}{2}(-3+2v+4v^2)-N_CvV_1\right)$$
$$\left.+\ln^2(v)\left(\frac{N_C}{2}(8-18v+17v^2)+C_F(3v^2+2v_1)\right)+\ln^2(v_1)\left(-\frac{N_C}{2}(1+v)v_1+C_F(1+v_1^2)\right)\right]\ ,$$

$$\tilde{c}_1=-\frac{T_{\gamma g}}{2}[b_0-2N_C\ln(v_1)+2N_C\ln(v)]\ ,$$

$$\tilde{\tilde{c}}_1=-\frac{C_FT_{\gamma g}}{4}[3+4\ln(v)]\ ,$$

$$\hat{c}_1=\frac{b_0T_{\gamma g}}{2}\ ,$$

$$c_2=\frac{T_{\gamma g}}{4}\left([C_F(-3+4\ln(v)]-4N_C[\ln(v_1)-3\ln(v)]\right)\ ,$$

$$\tilde{c}_2=-N_CT_{\gamma g}\ ,$$

$$\tilde{\tilde{c}}_2=-C_FT_{\gamma g}\ ,$$

$$c_3=(C_F+2N_C)T_{\gamma g}\ ,$$

$$c_5=\frac{N_C}{2}\left(\frac{-2(1+v)^2}{v_1^2}-\frac{2v(6-5v+2v^2)}{Xv_1}-\frac{2vv_1}{X^3}+\frac{2vv_2}{X^2}+\frac{6-13v+18v^2-11v^3+4v^4}{vv_1^2w}+\frac{2(1+3v^2)w}{v_1^2}\right)$$
$$+\frac{C_F}{2}\left(\frac{-2v}{X^2}-\frac{2v}{Y}-\frac{2(1+2v^2)}{v}+\frac{2vv_1}{X^3}+\frac{v(3-2vv_2)}{Xv_1}+\frac{3-2vv_1}{vw}-2\frac{(-v^2+2v^3-v_1)}{vv_1}w\right)\ ,$$

$$c_6=\frac{C_F}{v_1}\left(-v^2(2-w)-\frac{(1-2v)(v^2+v_2)}{vw}\right)+\frac{N_C}{2v_1^2}\left(v(7+v)-\frac{1+3v-2v^2v_1}{vw}-8v^2w\right)\ ,$$

$$c_7=\frac{N_C}{2vv_1w}(v_1+v^2w)-\frac{C_F}{Yvw}(Y+2v^2w)\ ,$$

$$c_8=-c_6-\frac{C_F}{v_1}\left(v^2(2-w)-\frac{(1+v^2)}{w}\right)-\frac{N_C}{2v_1}\left(-3v+\frac{3v^2+2v_1}{vw}\right)\ ,$$

$$c_9=\frac{N_C}{2}\left(-\frac{v(5+3v)}{v_1^2}-\frac{2v(1+v_1^2)}{Xv_1}+\frac{(2v^2+v_1)(2-vv_1)}{vv_1^2w}+\frac{8v^2w}{v_1^2}\right)-\frac{C_F}{vv_1w}(-v_1+v^2w+v^3w^2)\ ,$$

$$c_{10}=c_5+\frac{N_C}{2}\left(\frac{v}{v_1}+\frac{2v(1+v_1^2)}{Xv_1}+\frac{(-2+4v-3v^2+2v^3)}{vv_1w}\right)-\frac{C_F}{v_1w}[1+v^2(1-w)^2]\ ,$$

$$c_{11}=\frac{C_F}{2}\left(\frac{5v}{X^2}+\frac{2v}{Y}-\frac{6vv_1}{X^3}+\frac{(5-3vv_2)}{vv_1}+\frac{v(1+vv_3)}{Xv_1}+\frac{3-2v+6v^2}{2vw}-\frac{(v^2+2v^3+6v_1)w}{vv_1}\right)$$
$$+\frac{N_C}{2}\left(2-\frac{2v}{Y}+\frac{v(-7+2v)}{X^2}-\frac{v(-3+2v)}{Xv_1}+\frac{6vv_1}{X^3}+\frac{(1+v^2)}{v_1^2w}-\frac{2v_2w}{v_1}\right)$$

$$+\frac{\lambda}{2}\left[\frac{C_F}{vv_1}\left((3v^2-4v^3+2v_1)+\frac{2v^2v_1}{X^2}-\frac{2v^2v_1^2}{X^3}-\frac{v^2(3-2vv_2)}{X}-\frac{(1+v^2)v_1}{w}+(-2v^2+3v^3-2v_1)w\right)\right.$$
$$\left.-\frac{N_C}{v_1^2w}(1+v^2)(1-2w+2w^2)\right],$$
$$\tilde{c}_{11}=\frac{N_C}{2}\left(\frac{2vv_1}{X^3}-\frac{2vv_2}{X^2}+\frac{2v(4-vv_3)}{Xv_1}+\frac{2(1+3v^2)(1-w)}{v_1^2}-\frac{(2v^2+v_1)(v^2+v_2)}{vv_1^2w}\right)$$
$$+\frac{C_F}{2}\left(\frac{2v}{X^2}-\frac{(-3v^2+4v^3-2v_1)}{vv_1}-\frac{2vv_1}{X^3}-\frac{v(3-2vv_2)}{Xv_1}-\frac{1+v^2}{vw}+\frac{(-2v^2+3v^3-2v_1)w}{vv_1}\right),$$
$$c_{12}=-\left(C_F-\frac{N_C}{2}\right)\frac{1+2vv_1}{vv_1},$$
$$c_{13}=\frac{C_F}{vv_1}(1+v^2)+\frac{N_C}{2vv_1}(2-6v+5v^2),$$
$$c_{14}=\frac{N_C}{2vv_1}(1-4v+5v^2)+\frac{C_F}{vv_1}(1+v_1^2).$$

6. $\gamma g \to g + X$

$$c_1=0,\quad \tilde{c}_1=0,\quad \tilde{\tilde{c}}_1=0,\quad \hat{c}_1=0,\quad c_2=0,\quad \tilde{c}_2=0,\quad \tilde{\tilde{c}}_2=0,\quad c_3=0,$$
$$c_{12}=0,\quad c_{13}=0,\quad c_{14}=0,$$
$$c_5=C_F\left(\frac{-4v}{Y^2}+\frac{4vv_1}{X^2}-\frac{4(1-vv_1)}{v_1}-\frac{4v^2}{Yv_1v_2}-\frac{4v^2v_1}{Xv_2}+\frac{4(2v^2+v_1)}{v_1w}+\frac{4(1-vv_1)w}{v_1}\right)$$
$$+N_C\left(\frac{-2v^3}{Xv_2}+\frac{2v^3}{Yv_1v_2}-\frac{-2+4v-3v^2+v^3+2v^4}{v^2v_1w}\right)(1-2w+2w^2),$$
$$c_6=-\frac{2C_F(Y^2+v^2)}{v_1w},$$
$$c_7=-\frac{8C_Fv^2}{Y^2}(1-w),$$
$$c_8=N_C\left(\frac{2(1+v_1^2)}{Xv_2}-\frac{2(1+v_1^2)}{Yv_1v_2}+\frac{2-3vv_1}{vv_1w}\right)+2C_F\left(\frac{-2v}{v_1}-\frac{2(1+v_1^2)}{Xv_2}+\frac{2(1+v_1^2)}{Yv_1v_2}+\frac{v_1}{w}+\frac{2vw}{v_1}\right),$$
$$c_9=N_C\left(-2+\frac{2(1+v_1^2)}{Yv_1v_2}+\frac{2v_1(1+v_1^2)}{Xv_2}-\frac{2v^2+3v_1}{v_1w}\right)$$
$$+C_F\left(4-\frac{4(1+v_1^2)}{Yv_1v_2}-\frac{4v_1(1+v_1^2)}{Xv_2}+\frac{4(1-vv_1)}{v_1w}+\frac{2v^2w}{v_1}\right),$$
$$c_{10}=C_F\left(\frac{-4v}{Y^2}+\frac{4vv_1}{X^2}-\frac{8(1-vv_1)}{v_1}+\frac{8}{Yv_2}+\frac{8v_1^2}{Xv_2}+\frac{2(3v^2+2v_1)}{v_1w}+\frac{2(3v^2+2v_1)w}{v_1}\right)$$
$$+N_C\left(\frac{-4v_1}{v^2}-\frac{2(1+v_1^2)}{Xv_2}-\frac{2(1+v_1^2)}{Yv_2}+\frac{2v_1}{v^2w}+\frac{2(1+v_1^2)w}{v^2}\right),$$
$$c_{11}=N_C\left(\frac{4v}{Y^2}+\frac{2v^2}{X}+\frac{2v^2}{Yv_1}-\frac{4vv_1}{X^2}+\frac{2(v^2+6v_1)}{v^2}-\frac{2v^2+3v_1}{v_1w}-\frac{2(v^2+6v_1)w}{v^2}\right)+\frac{2C_F}{v_1w}(1+v_1^2+v^2w^2)$$
$$+\lambda\left[\frac{C_F}{v_1}\left(2(2-3v+2v^2)+\frac{4vv_1}{X}-\frac{4vv_1^2}{X^2}-\frac{3-4v+3v^2}{w}-(3v^2+4v_1)w\right)-\frac{N_C}{v^2w}(1+v_1^2)(1-2w+2w^2)\right],$$
$$\tilde{c}_{11}=\frac{C_F}{v_1}\left(2(2-3v+2v^2)+\frac{4vv_1}{X}-\frac{4vv_1^2}{X^2}-\frac{3-4v+3v^2}{w}-(3v^2+4v_1)w\right)-\frac{N_C}{v^2w}(1+v_1^2)(1-2w+2w^2),$$
$$\tilde{\tilde{c}}_{11}=-\frac{C_F}{Y^2v_1w}[1+v^2(1-w)^2](v_1^2+v^2w^2).$$

7. $\gamma q \to \bar{q} + X$

$$c_1 = 0,\quad \tilde{c}_1 = 0,\quad \tilde{\tilde{c}}_1 = 0,\quad \hat{c}_1 = 0,\quad c_2 = 0,\quad \tilde{c}_2 = 0,\quad \tilde{\tilde{c}}_2 = 0,\quad c_3 = 0\ ,$$

$$c_{12} = 0,\quad c_{13} = 0,\quad c_{14} = 0\ ,$$

$$c_5 = \frac{C_F}{2}\left(\frac{v}{X^2} + \frac{(3-2v)v}{Y} - \frac{vv_1}{Y^2} - \frac{vv_3}{Xv_1} - 4(2v^4 + 5v^2v_1 + v_1^2)\frac{1-w}{v_1^2} + \frac{4(v^4 + 3v^2v_1 + v_1^2)}{v_1^2 w}\right)$$
$$-\frac{C_F v^2}{N_C v_1 w}(1 - 2w + 2w^2)\ ,$$

$$c_6 = \frac{C_F}{2v_1^2}\left(2v(2 + vv_3) - \frac{2(1+v^2)}{w} - 4v^2v_3 w\right)\ ,$$

$$c_7 = \frac{C_F}{2}\left(\frac{2(3-2v)v}{Y} - \frac{2(2-3v)v}{v_1} - \frac{2vv_1}{Y^2} - \frac{4v^2 w}{v_1}\right)\ ,$$

$$c_8 = \frac{C_F}{2N_C}\left(\frac{-2(v^2+2v_1)}{Y} + \frac{2(v^2+2v_1)}{Xv_1} + \frac{2v^2(1-2w)}{v_1 w} - 8vw\right) + \frac{C_F}{2v_1^2}\left(-4v^2v_3 + \frac{2(1+v^2)}{w} - 8v(1 - vv_3)w\right)\ ,$$

$$c_9 = \frac{C_F}{v_1^2}\left(-(4v^2 - v_1)(1+v_1^2) + \frac{2(v^4 + 3v^2v_1 + v_1^2)}{w} + 2v^2(2v^2 + v_1)w + 8v^2v_1w^2\right)$$
$$+\frac{C_F v^2}{N_C v_1}(1 - 2w + 2w^2)\left(\frac{1}{X} + \frac{1}{w} + \frac{v_1}{(v_1 + vw)}\right)\ ,$$

$$c_{10} = c_5 + \frac{C_F v^2}{N_C v_1}\left(\frac{v}{Xv_2} - \frac{vv_1}{Yv_2} + \frac{1}{w}\right)(1-2w)(1-2w+2w^2) - \frac{C_F}{v_1}(5v^2 + 2v_1 - 10v^2w + 8v^2w^2)\ ,$$

$$c_{11} = \frac{C_F v^2}{N_C v_1 w} + \frac{C_F}{2v_1^2}\left(\frac{v(2+v)v_1}{X} - \frac{2vv_1^2}{X^2} - \frac{(2-3v)vv_1^2}{Y} + \frac{2vv_1^3}{Y^2} + 4(2 - 4vv_1 - v^3v_2) + \frac{2v_1^2}{w} - 2(2v^4 + 5v^2v_1 + 8v_1^2)w\right)$$
$$+\lambda\left[\frac{C_F}{2v_1}\left(\frac{vv_1}{X^2} - \frac{vv_3}{X} + 4(v_1 + v^2v_2)(1-w) - \frac{v_1(v^2+v_1^2)}{w}\right) - \frac{C_F v^2}{N_C v_1 w}(1 - 2w + 2w^2)\right]\ ,$$

$$\tilde{c}_{11} = \frac{C_F}{2v_1^2}\left(-\frac{vv_1^2}{X^2} + \frac{vv_1v_3}{X} - 4(4v^2 - 3v^3 + v^4 + v_1^2)(-1+w) - \frac{3 - 4v + 9v^2 - 2v^3v_3}{w}\right) - \frac{C_F v^2}{N_C v_1 w}(1 - 2w + 2w^2)\ ,$$

$$\tilde{\tilde{c}}_{11} = \frac{C_F}{2}\left(-\frac{(3-2v)v}{Y} + \frac{vv_1}{Y^2} + 4v^2(1-w) - \frac{v^2 + v_1^2}{w}\right)\ .$$

8. $\gamma q \to q' + X$

$$c_1 = 0,\quad \tilde{c}_1 = 0,\quad \tilde{\tilde{c}}_1 = 0,\quad \hat{c}_1 = 0,\quad c_2 = 0,\quad \tilde{c}_2 = 0,\quad \tilde{\tilde{c}}_2 = 0,\quad c_3 = 0\ ,$$

$$c_{12} = 0,\quad c_{13} = 0,\quad c_{14} = 0\ ,$$

$$c_5 = C_F\left[e_q'^2\left(\frac{v}{2X^2} - \frac{vv_3}{2Xv_1} - \frac{(1+3v^2)(1-w)}{v_1^2} + \frac{1+v^2}{v_1^2 w}\right)\right.$$
$$\left.+e_q^2\left(\frac{(3-2v)v}{2Y} - \frac{vv_1}{2Y^2} - (3v^2 + v_1^2)(1-w) + \frac{1 - 2vv_1}{w}\right)\right]\ ,$$

$$c_6 = C_F\left[\frac{e_q e_q' v^2(1-2w)}{v_1} + \frac{e_q'^2}{v_1^2}\left(2v(1+v) - \frac{1+v^2}{w} - 4v^2 w\right)\right]\ ,$$

$$c_7 = C_F\left(e_q e_q' v^2 \frac{1-2w}{v_1} - e_q^2 v^2 w \frac{1 - 2v + 2vw}{Y^2}\right)\ ,$$

$$c_8 = C_F\left[2e_q e_q' v(1-2w) + \frac{e_q'^2}{v_1^2}\left(-2v(1+v) + \frac{1+v^2}{w} + 4v^2 w\right)\right]\ ,$$

$$c_9 = C_F\left(\frac{e_q^2}{w}[1-2vv_1+2vw-4v^2(1-w)w]+\frac{e_q'^2}{v_1^2 w}(1+v^2-2vw-2v^2w+4v^2w^2)\right.$$
$$\left.+\frac{e_q e_q'}{v_1}(3v^2+2v_1-6v^2w+8v^2w^2)\right),$$

$$c_{10} = C_F\left[\frac{e_q'^2}{2}\left(\frac{v}{X^2}-\frac{vv_3}{Xv_1}-\frac{2(1+3v^2)(1-w)}{v_1^2}+\frac{2(1+v^2)}{v_1^2 w}\right)+\frac{e_q^2}{2}\left(\frac{(3-2v)v}{Y}-\frac{vv_1}{Y^2}\right.\right.$$
$$\left.\left.-2(3v^2+v_1^2)(1-w)+\frac{2(v^2+v_1^2)}{w}\right)-\frac{e_q e_q'}{v_1}(5v^2+2v_1-10v^2w+8v^2w^2)\right],$$

$$c_{11} = C_F\left\{e_q e_q'\left(2-\frac{v}{X}+\frac{v}{Y}-4w\right)+e_q^2\left(-1+2v^2+\frac{v(-4+3ev)}{2Y}+\frac{vv_1}{Y^2}+\frac{3}{2w}-v(-1+2v)w\right)\right.$$
$$+\frac{e_q'^2}{2}\left(\frac{-2v}{X^2}+\frac{2(2v^2+v_1^2)}{v_1^2}+\frac{vv_4}{Xv_1}+\frac{1}{w}-\frac{2(2-3vv_1)w}{v_1^2}\right)$$
$$\left.+\lambda\left[-\frac{e_q^2}{2w}[(1-2vv_1)(1-2w+2w^2)]+\frac{e_q'^2}{2v_1}\left(\frac{vv_1}{X^2}-\frac{vv_3}{X}-2(1+v)(-1+w)\right)\right]\right\},$$

$$\tilde{c}_{11} = C_F\left[\frac{e_q'^2}{2}\left(-\frac{v}{X^2}+\frac{vv_3}{Xv_1}+\frac{2(1+3v^2)(1-w)}{v_1^2}-\frac{2(1+v^2)}{v_1^2 w}\right)-\frac{e_q^2}{2w}[(1-2vv_1)(1-2w+2w^2)]\right],$$

$$\tilde{\tilde{c}}_{11} = \frac{C_F e_q^2}{2}\left(-\frac{(3-2v)v}{Y}+\frac{vv_1}{Y^2}+4v^2(1-w)-\frac{v^2+v_1^2}{w}\right).$$

[1] AMY Collaboration, R. Tanaka *et al.*, Phys. Lett. B **277**, 215 (1992); TOPAZ Collaboration, H. Hayashii *et al.*, *ibid.* **314**, 149 (1993).

[2] H1 Collaboration, T. Ahmed *et al.*, Phys. Lett. B **297**, 404 (1992).

[3] A. C. Bawa, M. Krawczyk, and W. J. Stirling, Z. Phys. C **50**, 293 (1991).

[4] P. Aurenche, P. Chiappetta, M. Fontannaz, J. Ph. Guillet, and E. Pilon, Z. Phys. C **56**, 589 (1993).

[5] L. E. Gordon and J. K. Storrow, Z. Phys. C (to be published).

[6] R. Barndelik *et al.*, Phys. Lett. **107B**, 290 (1981).

[7] M. Althoff *et al.* Phys. Lett. **138B**, 219 (1984).

[8] D. Cords *et al.*, Phys. Lett. B **302**, 341 (1993).

[9] M. Drees and R. Godbole, Phys. Rev. Lett. **61**, 682 (1988); Phys. Rev. D **39**, 169 (1989).

[10] L. E. Gordon and J. K. Storrow, Phys. Lett. B **291**, 305 (1992).

[11] M. Greco and A. Vicini, Nucl. Phys. **B415**, 386 (1994).

[12] L. E. Gordon, Nucl. Phys. **B419**, 25 (1994).

[13] J. Chyla, Phys. Lett. B **320**, 186 (1993).

[14] P. Aurenche *et al.*, Phys. Lett. **135B**, 164 (1984); Nucl. Phys. **B286**, 553 (1987).

[15] P. Aurenche, R. Baier, A. Douiri, M. Fontannaz, and D. Schiff, Z. Phys. C **29**, 423 (1985).

[16] F. Aversa, P. Chiapetta, M. Greco, and J. Ph. Guillet, Phys. Lett. B **210**, 225 (1988); **211**, 465 (1988); Nucl. Phys. **B327**, 105 (1989).

[17] F. M. Borzumanti, B. A. Kniehl, and G. Kramer, Z. Phys. C **59**, 341 (1993).

[18] B. A. Kniehl and G. Kramer, Z. Phys. **62**, 53 (1994).

[19] P. Chiappetta, M. Greco, J. Ph. Guillet, S. Rolli, and M. Werlen, Nucl. Phys. **B412**, 3 (1994).

[20] M. Glück, E. Reya, and A. Vogt, Z. Phys. C **53**, 127 (1992).

[21] M. Glück, E. Reya, and A. Vogt, Phys. Rev. D **45**, 3986 (1992).

[22] L. E. Gordon and J. K. Storrow, Z. Phys. C **56**, 307 (1992).

[23] C. F. von Weizsäcker, Z. Phys. **88**, 612 (1934); E. J. Williams, Phys. Rev. **45**, 729 (1934).

[24] A. C. Bawa and W. J. Stirling, J. Phys. G **15**, 1339 (1989).

[25] D. Amati, R. Petronzio, and G. Venezanio, Nucl. Phys. **B146**, 29 (1978); A. H. Mueller, Phys. Rev. D **18**, 3705 (1978); S. Libby and G. Sterman, *ibid.* **18**, 3252 (1978); R. K. Ellis, M. Machacek, H. D. Politzer, and G. G. Ross, Nucl. Phys. **B152**, 285 (1979).

[26] G. Altarelli and G. Parisi, Nucl. Phys. **B126**, 298 (1977).

[27] J. F. Owens, Rev. Mod. Phys. **59**, 465 (1987).

[28] M. Drees and R. Godbole, Nucl. Phys. **B339**, 335 (1990).

[29] G.'t Hooft and M. Veltman, Nucl. Phys. **B44**, 189 (1972).

[30] W. A. Bardeen, A. J. Buras, D. W. Duke, and T. Muta, Phys. Rev. D **18**, 3998 (1978).

[31] F. A. Berends, Z. Kunszt, and R. Gastmans, Phys. Lett. **92B**, 186 (1980); Nucl. Phys. **B182**, 397 (1981).

[32] F. Khalafi, P. V. Landshoff, and W. J. Stirling, Phys. Lett. **130B**, 215 (1983).

[33] D. Bödecker, Z. Phys. C **59**, 501 (1993).

[34] M. A. Nowak, M. Praszalowicz, and W. Slominski, Ann. Phys. (N.Y.) **166**, 443 (1986).

[35] L. E. Gordon and W. Vogelsang, Phys. Rev. D **48**, 3136 (1993).

[36] R. K. Ellis, M. A. Furman, H. E. Haber, and I. Hinchliffe, Nucl. Phys. **B173**, 397 (1980).

[37] The matrix elements can be obtained in FORTRAN form

upon request from GORDON@HEP.ANL.GOV.
[38] A. D. Martin, W. J. Stirling, and R. G. Roberts, Phys. Lett. B **306**, 145 (1993).
[39] R. Baier, J. Engels, and B. Petersson, Z. Phys. C **2**, 265 (1979); M. Anselmino, P. Kroll, and E. Leader, *ibid.* **18**, 307 (1983).
[40] J. Binnewies, B. A. Kniehl, and G. Kramer (private communication).